

A Survey on Human Interaction Motion Generation

Kewei Sui¹ · Anindita Ghosh*² · Inwoo Hwang*³ · Bing Zhou¹ ·
Jian Wang¹ · Chuan Guo¹

Received: xx Mar 2025 / Accepted: xx xx 2025

Abstract Humans inhabit a world defined by interactions—with other humans, objects, and environments. These interactive movements not only convey our relationships with our surroundings but also demonstrate how we perceive and communicate with the real world. Therefore, replicating these interaction behaviors in digital systems has emerged as an important topic for applications in robotics, virtual reality, and animation. While recent advances in deep generative models and new datasets have accelerated progress in this field, significant challenges remain in modeling the intricate human dynamics and their interactions with entities in the external world. In this survey, we present, *for the first time*, a comprehensive overview of the literature in human interaction motion generation. We begin by establishing foundational concepts essential for understanding the research background. We then systematically review

existing solutions and datasets across three primary interaction tasks—human-human, human-object, and human-scene interactions—followed by evaluation metrics. Finally, we discuss open research directions and future opportunities. The repository listing relevant papers is accessible at: <https://github.com/soraproducer/Awesome-Human-Interaction-Motion-Generation>.

Keywords Human Interaction · Motion Generation · Deep Learning · Literature Survey

1 Introduction

Human life is fundamentally characterized by interactions with the external environment through motion [35,159]. These interactions range from everyday actions, such as using a smartphone and cooking, to social gestures, such as handshakes and clapping. Successfully understanding and reproducing such complex behaviors is crucial for developing human-like entities across various domains, including 3D virtual characters in entertainment media [9,220], humanoid robots [102,156], and digital avatars [11,110,218].

The past decade has witnessed remarkable progress in generative modeling across multiple domains: text [18,176,211], images [98,177,178], video [190,214,223], audio [44,86,216], and 3D objects [149,161,236]. This advancement has been driven by foundational generative models, including Variational Autoencoders (VAEs) [103], Generative Adversarial Networks (GANs) [66], Diffusion models [38,252], Large Language Models (LLMs) [150], and Vision-Language Models (VLMs) [123]. These developments have also enhanced our ability to generate diverse and natural 3D human motions from various inputs such as action categories

Kewei Sui
E-mail: ksui@snapchat.com

Anindita Ghosh
E-mail: anindita.ghosh@dfki.de

Inwoo Hwang
E-mail: inwoohwang0818@gmail.com

Bing Zhou
E-mail: bzhou@snapchat.com

Jian Wang
E-mail: jwang4@snapchat.com

Chuan Guo
E-mail: cguo2@snapchat.com

¹ Snap Inc., California, USA

² Saarland Informatics Campus, DFKI, MPI Informatics, Germany

³ Seoul National University, Seoul, South Korea

* Indicates equal contribution

(Corresponding author: Chuan Guo)

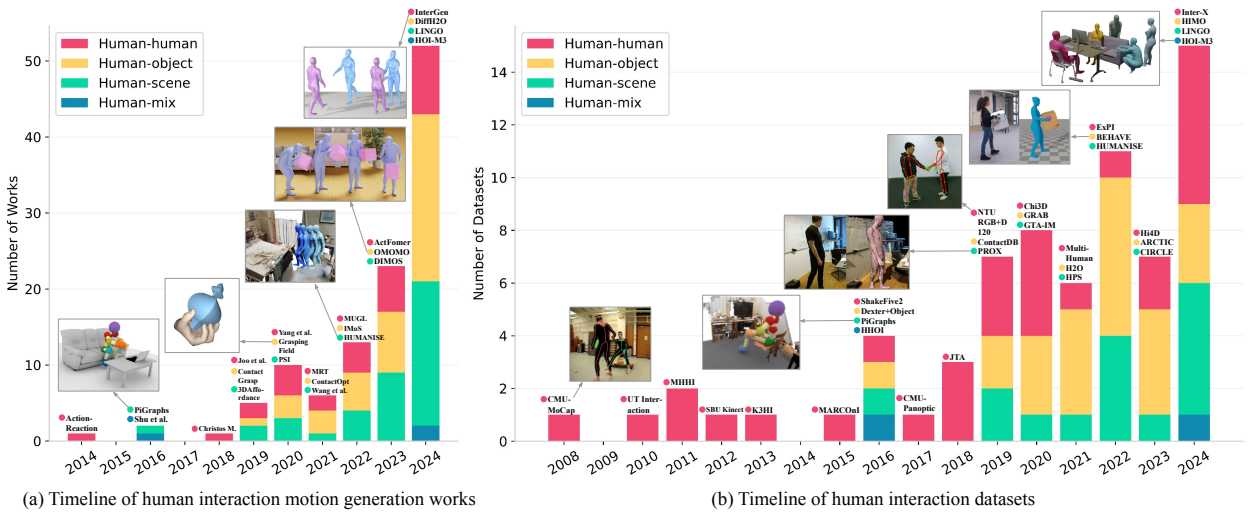


Fig. 1: Statistics on the number of works and datasets on human interaction motion generation over the past two decades, categorized into four interaction scenarios.

[69, 136, 165], textual descriptions [29, 67, 99, 166, 209, 262], audio [7, 63, 121, 192, 213], and so on.

However, generating human *interaction* motions presents distinct challenges beyond standard generative modeling approaches. First, human interaction is inherently stochastic, yet the resulting body movements must maintain spatial and temporal coherence that aligns with specific human intentions. Second, interacting with the external world demands environmental awareness, requiring adaptation to diverse scene layouts, understanding of object properties and affordances, and compliance with physical constraints to prevent intra- and inter-penetration. Last but not least, the collection of human interaction data is resource-intensive and difficult to scale, making it impractical to rely solely on data-driven learning. Therefore, incorporating domain expertise into learning models is essential to complement traditional generative methods. In summary, generating natural human interaction motions requires the ability to model human dynamics, incorporate physical constraints, and understand the spatial semantics and relationships within the holistic environment.

Despite these challenges, research on human interaction generation has advanced rapidly in the last decade, with growing interest over time. Fig. 1 chronicles these developments, highlighting key milestones covered in this survey. We categorize human interaction scenarios in existing motions into four main types: human-human interaction (HHI), human-object interaction (HOI), human-scene interaction (HSI), and human-mix interaction (involving multiple interaction types simultaneously). This survey provides a comprehensive review of interactive human motion generation, addressing recent advances and emerging challenges. The paper is structured as fol-

lows. In Section §2, we define the scope of this survey and identify related topics beyond its scope. Section §3 covers the preliminaries, providing foundational knowledge and key concepts essential for understanding the subsequent sections. Section §4 reviews the various methods and techniques employed in interactive human motion generation. In Section §5, we provide an overview of the commonly used datasets in this field, highlighting their distinct features. Section §6 explores the evaluation metrics utilized to measure the performance of these methods. Finally, Section §7 summarizes the current landscape and offers an exploration of future research directions. This survey aims to provide researchers and practitioners with a comprehensive understanding of the state of the art in this rapidly evolving field.

2 Scope

This survey examines interactive human motion generation, with a focus on generation methods, datasets, and evaluation metrics across four key interaction types illustrated in Fig. 2: human-human, human-object, human-scene, and human-mix interactions. Our investigation encompasses various generation approaches, including interactive motion generation, motion prediction, and physics-based simulation. The scope of this survey specifically excludes human motion tasks that do not involve generation or interactions. Related but distinct research areas include single-person motion generation [285], human motion style transfer [6], human pose estimation [30, 129], and human action recognition [105]. For comprehensive reviews of these topics, the readers can refer to the respective surveys cited above.

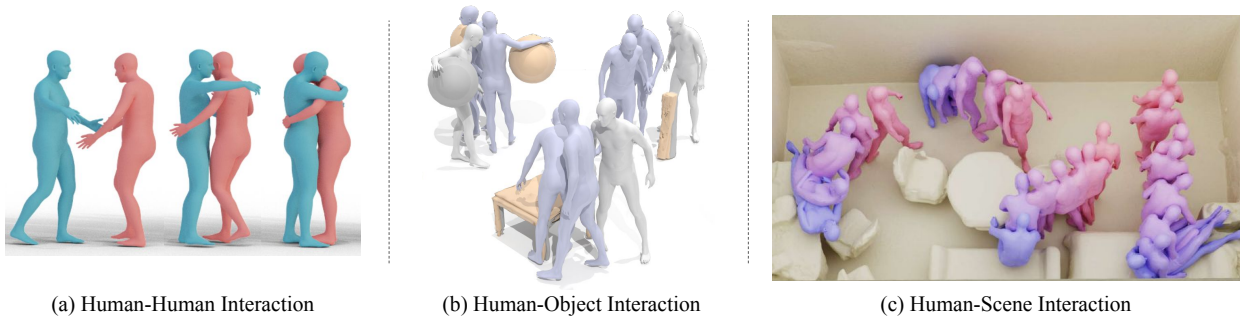


Fig. 2: Illustration of three major human interaction motion generation tasks: (a) Human-human Interaction; (b) Human-object Interaction; and (c) Human-scene Interaction. Figures are adapted from [95, 244, 247].

3 Preliminaries

This section establishes the fundamental concepts of human interaction motion generation. We examine three key aspects: the entities involved in interactions, the conditions governing interaction motions, and the core methodologies for generating these motions. This foundation provides essential context for understanding the research developments discussed throughout the survey.

3.1 Interactive Entities

3.1.1 Human Motion

Human motion is a fundamental component of interactions. Accurate motion capture and efficient motion representation are essential for human interaction motion generation models.

Human Motion Capture. Human movements can be captured through several approaches, each with distinct trade-offs. Marker-based optical systems (e.g., Vicon [146] and OptiTrack [55]) track markers attached to key joints using multiple optical cameras, providing the highest precision but at a significant cost. Inertial-based motion capture systems offer an affordable alternative using IMU sensors or Smartsuits [147] to track body segment movements, although they require regular calibration to address sensor drift. RGB-D cameras (e.g., Kinect [273]) enable low-cost motion capture through single or multi-view setups, extracting 3D joint information from RGB and depth data, but typically lack fine motion details. Recent deep learning-based pose estimation methods [104, 232] can reconstruct 3D motions from video footage, although their generalization capabilities remain limited. Additionally, 3D graphics engines provide a flexible option for generating synthetic human motions in a virtual 3D environment, without physical capture equipment.

Representation. In kinematic-based methods, human motion is represented as a sequence of skeletal poses defined by joints or bones in 3D space. These motions can be expressed through either 3D joint positions or bone rotations along kinematic chains (e.g., limbs and spine). Recent studies [222, 284] favor rotation-based representations as they inherently encode skeletal topology. While traditional rotation formats (Euler angles and quaternions) are available, the 6D rotation representation [284] has gained prominence for its continuity and compatibility with deep learning models. Parametric models such as SMPL [134], SMPL-X [163], and GHUM [243] extend beyond rotational pose parameters by incorporating shape parameters. These models parameterize surface vertices and deformations using both pose and shape information, enabling geometry-aware motion representation, which is crucial for fine-grained interactions.

3.1.2 Object

Objects also serve as important interactive entities. Capturing their shape and motion accurately, along with structured representation, is essential for object-centric interaction modeling.

Object Shape and Motion Capture. To capture both the shape and motion of 3D objects, several complementary approaches are typically used. For shape capture, methods include 3D scanning (using laser scanners [48], structured light [265], or photogrammetry [199]), RGB-D sensors [286], or multi-view stereo reconstruction [183]. Object motion can be tracked either using marker-based approaches, where reflective markers are attached to key points and tracked with optical motion capture systems, or through markerless methods that rely on visual feature tracking [187], dense surface tracking [157], or deep learning-based pose estimation [239]. Articulated objects require additional consideration. The first step typically involves modeling the object’s kinematic struc-

ture, defining joint hierarchies, and establishing articulation constraints. Capture typically involves tracking individual rigid segments using markers placed at joints and key points, followed by articulation reconstruction from marker trajectories [94]. To ensure realistic dynamics, these captured motions are often enhanced with physics-based simulations that model collision responses, gravitational effects, and inertial forces [228, 231, 270].

Representation. In human-object interaction synthesis, objects are represented in various formats to capture their geometric and physical attributes for deep learning models. Point clouds capture object surfaces as unordered 3D points, offering flexibility for complex shape modeling [71]. Meshes provide high-resolution geometric details through vertices and edges, enabling precise contact modeling. Basis Point Sets (BPS) [170] encode object geometry in fixed-dimensional representations, balancing efficient neural processing with robustness to shape variations. For rigid objects in motion, the 6 Degrees of Freedom (6DoF) format represents both translation and orientation as $\mathbf{T}1 : N = [\mathbf{t}, \mathbf{R}]1 : N$, where N is the total frame count, $\mathbf{t} \in \mathbb{R}^3$ denotes translation, and $\mathbf{R} \in SO(3)$ represents rotation at each frame. Articulated objects [53] are modeled using a 3D mesh $\mathcal{O}(\Omega) \in \mathbb{R}^{V \times 3}$, where V represents the count of vertices on the object surface. The object pose $\Omega \in \mathbb{R}^7$ combines articulation rotation ($\omega \in \mathbb{R}$), object translation $\mathbf{t} \in \mathbb{R}^3$, and object rotation $\mathbf{R} \in SO(3)$. These representations are often enhanced with object-centric interaction regions and canonicalization techniques to standardize spatial relationships.

3.1.3 Scene

Scenes provide the spatial and contextual foundation for interactions, necessitating accurate acquisition methods and structured representations to model human-scene relationships effectively.

Scene Acquisition. Human-scene interactions can be captured in both real and virtual environments. Real-world scenes are digitized using advanced scanning technologies: LiDAR systems capture high-resolution 3D point clouds [36], while structured light scanning [79, 101] reconstructs detailed surface geometry. Alternatively, existing 3D scene datasets, such as ScanNet [40], provide ready-to-use virtual environments [234]. Recent approaches have expanded scene diversity through synthetic virtual environments [8, 21, 93, 95]. Created using 3D modeling tools like Unity [171], Unreal Engine [126], or Blender [43], these environments offer precise control over scene parameters, including textures, lighting,

and object placement. This approach enables the scalable capture of complex human-scene interactions across diverse settings.

Representation. Point clouds are widely used due to their lightweight nature and their ability to preserve detailed geometric information. Each point contains the 3D spatial coordinates of scene surfaces, with additional features like surface normals or semantic labels. These representations are typically processed using specialized architectures, like PointNet [173] or PointTransformer [275]. Occupancy grids and voxel representations discretize 3D space into regular cells containing binary information. These approaches facilitate efficient collision checking and spatial reasoning, making them particularly valuable for human-scene interaction tasks. Various architectures, including 3D Convolutional Networks (3D-CNNs) [212] and Vision Transformers (ViTs) [47], have been employed to process these representations. Similar to object representation, BPS [170] features also offer a structured encoding of scene geometry by measuring point-wise distances to a predefined set of basis points.

3.2 Conditioning Modalities

Human interaction motion synthesis often conditions on other modalities. These modalities provide additional context or constraints, enabling more controllable and semantically consistent motion generation.

Text Textual descriptions have emerged as a popular modality for guiding human interaction motion generation [52, 124, 148, 169, 184, 185, 235, 250]. Text-based guidance enables models to process detailed instructions that define interactions between generated human motions and various entities (humans, objects, scenes, or combinations thereof). These text conditions are typically incorporated either as embeddings—such as CLIP [175] embeddings [52, 148, 169, 184, 185, 235]—as penultimate layer outputs from LLMs [124], or as sequences of discrete word tokens [250].

Audio Audio-driven approaches enable models to generate interaction motions synchronized with acoustic cues, typically in HHI scenarios [5, 191, 253]. The audio input manifests either as conversational exchanges between actors and reactors [5, 253] or as musical accompaniment [191] coordinating multiple participants. These acoustic signals are processed into salient features—including prosody, excitation, music intensity, and rhythmic beats—using established tools such as OpenSmile [50] and Librosa [143].

Action Class Action classes serve as a well-established conditioning mechanism in human inter-

action motion generation [61, 72, 138, 245]. These categorical descriptors are typically implemented as one-hot encodings [61, 72, 138] or label token embeddings [59, 245], representing basic interactions such as "Shake Hands" or "Combat".

Spatial and Temporal Signal Diverse spatial signals guide interactive motion generation, encompassing goal poses [34, 116, 202, 258, 277], root trajectory [17, 130, 215, 283], root positions [8, 111], orientations [235], object motions [118], and gamepad signals (e.g., instant direction, speed) [195, 197, 198]. These explicit, deterministic signals provide precise control over generated motions, enhancing both accuracy and adaptability while preserving motion fidelity.

3.3 Fundamental Methods for Interaction Synthesis

In this subsection, we introduce fundamental methods used in human interaction motion generation, ranging from classical approaches to the latest deep generative frameworks.

3.3.1 Motion Graph

Graph-based methods [106] represent a foundational approach in human interaction motion generation [4, 87, 154, 253], leveraging the inherent structure of motion data to synthesize novel sequences. These approaches typically implement motion graphs—directed graphs where nodes represent motion segments or poses, and edges denote viable transitions between segments. Novel motion synthesis occurs through graph traversal, where random walks along connected nodes generate coherent motion sequences. This framework enables the combinatorial fusion of characteristics from multiple exemplars, producing diverse motions while preserving the authenticity of the source data. However, graph-based methods exhibit inherent limitations [106] in scalability. The approach necessitates storing the complete dataset and performing graph traversal during inference, introducing undesirable computational and storage overhead.

3.3.2 Deterministic Regression

Deterministic regression models [3, 12, 109] formulate interactive motion generation as a one-to-one mapping problem, predicting deterministic target motions from specified input conditions, typically supervised by L1 or L2 losses. These architectures commonly employ RNN [31, 180], or Transformer [219] backbones to capture temporal dependencies via autoregressive regression. Nevertheless, their one-to-one mapping paradigm fails

to capture the inherent stochasticity of human motions, often leading to mean poses and lifeless motions.

3.3.3 Generative Adversarial Networks

Generative Adversarial Networks (GANs) [64] have been commonly used for human interaction motion generation [61, 145, 245]. The GAN architecture comprises two key components: a generator (G) and a discriminator (D). The generator (G) transforms random noise vectors sampled from a standard normal distribution ($\mathbf{z} \sim \mathcal{N}(\mathbf{0}, \mathbf{I})$) into interaction motions ($G(\mathbf{z})$). Meanwhile, the discriminator (D) evaluates the authenticity of the generated motions by learning to differentiate between real human motion samples (\mathbf{x}) from the training distribution and synthetic samples produced by G . This adversarial dynamic is formalized through the following objective function:

$$\min_G \max_D \left[\mathbb{E}_{\mathbf{x} \sim p_{\text{data}}(\mathbf{x})} (\log D(\mathbf{x})) + \mathbb{E}_{\mathbf{z} \sim p_{\mathbf{z}}(\mathbf{z})} (\log(1 - D(G(\mathbf{z}))) \right], \quad (1)$$

where $p_{\text{data}}(\mathbf{x})$ represents the distribution of real human motion data and $p_{\mathbf{z}}(\mathbf{z})$ denotes the prior distribution of the noise vector \mathbf{z} . The generator seeks to minimize this objective by producing motions that the discriminator cannot reliably distinguish from real data, while the discriminator aims to maximize its ability to correctly classify real and generated motions.

Despite their impressive generative capabilities, GANs present training challenges [66]. The inherent instability of adversarial training manifests itself in several critical issues: mode collapse, where the generator converges to produce only a limited subset of possible motions, and convergence problems, where the generator-discriminator dynamics fails to reach a stable equilibrium.

3.3.4 Variational Autoencoders

Variational Autoencoders (VAEs) [103] employ a two-stage architecture: first encoding input data into a structured latent space, then sampling from this learned distribution to reconstruct the original data. By maximizing the Evidence Lower Bound (ELBO), VAEs approximate the intractable log-likelihood of the data distribution. The ELBO for a VAE is expressed as:

$$L_{\theta, \phi}(\mathbf{x}) = \mathbb{E}_{\mathbf{z} \sim q_{\phi}(\mathbf{z}|\mathbf{x})} [\ln p_{\theta}(\mathbf{x}|\mathbf{z})] - D_{KL}(q_{\phi}(\mathbf{z}|\mathbf{x}) \parallel p_{\theta}(\mathbf{z})), \quad (2)$$

where \mathbf{x} represents the input data, \mathbf{z} denotes the latent variables, θ and ϕ are the parameters of the decoder and

encoder networks respectively, $q_\phi(\mathbf{z}|\mathbf{x})$ is the approximate posterior, and $p(\mathbf{z})$ is the prior distribution over the latent variables.

Conditional Variational Autoencoders (cVAEs) [193] extend the VAE framework by incorporating conditioning variables, enabling controlled data generation based on specific attributes. In human interaction motion synthesis, cVAEs have demonstrated versatility through various conditioning approaches: motion class labels [59, 72, 120, 138], textual descriptions [148, 249], target poses [130, 215], and other control signals. The ELBO formulation is accordingly modified to incorporate the conditioning variable \mathbf{c} :

$$\mathcal{L}_{\theta, \phi}(\mathbf{x}|\mathbf{c}) = \mathbb{E}_{\mathbf{z} \sim q_\phi(\mathbf{z}|\mathbf{x}, \mathbf{c})} [\ln p_\theta(\mathbf{x}|\mathbf{z}, \mathbf{c})] - D_{\text{KL}}\left(q_\phi(\mathbf{z}|\mathbf{x}, \mathbf{c}) \parallel p_\theta(\mathbf{z}|\mathbf{c})\right), \quad (3)$$

where \mathbf{c} represents the conditioning information.

3.3.5 Diffusion Models

Diffusion models [83] have emerged as an expressive framework for generative modeling, demonstrating the capability to capture the complex data distribution in interactive human motions [23, 33, 52, 60, 93, 185, 233, 255, 264]. The framework consists of two key processes: a forward diffusion process that systematically corrupts data with Gaussian noise across multiple timesteps until reaching a standard Gaussian distribution, and a learned reverse process that progressively denoises the corrupted data to reconstruct realistic human motions. The forward diffusion process is formally expressed as:

$$q(\mathbf{x}_t|\mathbf{x}_{t-1}) = \mathcal{N}(\mathbf{x}_t; \sqrt{1 - \beta_t}\mathbf{x}_{t-1}, \beta_t\mathbf{I}), \quad (4)$$

where β_t represents the variance schedule at timestep t , and \mathcal{N} denotes a Gaussian distribution. The reverse denoising process is modeled as:

$$p_\theta(\mathbf{x}_{t-1}|\mathbf{x}_t) = \mathcal{N}(\mathbf{x}_{t-1}; \mu_\theta(\mathbf{x}_t, t), \Sigma_\theta(\mathbf{x}_t, t)), \quad (5)$$

where μ_θ and Σ_θ are the mean and covariance predicted by the neural network parameterized by θ .

In contrast to GANs’ single-step adversarial approach, the gradual, multi-step training dynamics of diffusion models provides inherent stability, enabling them to capture fine-grained motion details while maintaining diversity in their outputs.

3.3.6 Transformer-Based Language Models

Transformers [219] leverage self-attention mechanisms to efficiently capture long-range dependencies within

data sequences. Introduced by Vaswani et al. [219], the core self-attention equation is defined as:

$$\text{Attention}(Q, K, V) = \text{softmax}\left(\frac{QK^\top}{\sqrt{d_k}}\right)V, \quad (6)$$

where Q , K , and V are the query, key, and value matrices derived from input embeddings, and d_k is the dimensionality of the key vectors. This mechanism allows the model to dynamically focus on relevant parts of the input sequence when generating each output element.

Transformer-based language models, including GPTs [2, 18] and generative masked transformers [24], also become a promising paradigm for interaction motion modeling [91, 191]. These approaches typically implement a three-phase architecture: first, discretizing continuous motion data into tokens using encoders, like Vector Quantized Variational Autoencoders (VQ-VAEs) [217], which preserve essential motion structure and dynamics; second, modeling the sequential relationships between these tokens using transformer-based language models; and finally, projecting the tokenized representations back into continuous 3D motion sequences through a VQ-VAE decoder.

3.3.7 RL + Physics Simulation

Reinforcement Learning (RL) combined with physics simulation aims to generate more physically plausible interactive human motions [34, 80, 160, 229, 240, 258]. This approach leverages RL’s ability to learn optimal policies through trial-and-error while utilizing physics simulators to ensure that the generated motions adhere to fundamental physical laws. In this framework, an RL agent interacts with a physics-based environment, guided by rewards that promote target behaviors while accounting for constraints such as balance and collisions with objects or scenes. The design of reward functions plays a critical role in these approaches. On the one hand, RL-based methods often face training convergence challenges and exhibit limited generalization to novel actions. On the other hand, physics-based simulation remains essential as human motions inherently follow physical constraints in the real world—a fundamental aspect that purely kinematic-based methods struggle to capture.

3.3.8 LLM-Based Motion Planning

Recent advances in Large Language Models (LLMs) [150] have enabled their application as automated motion planners [32, 240, 248], translating high-level interaction goals into detailed step-by-step motion sequences. These approaches innovate by generating interactions

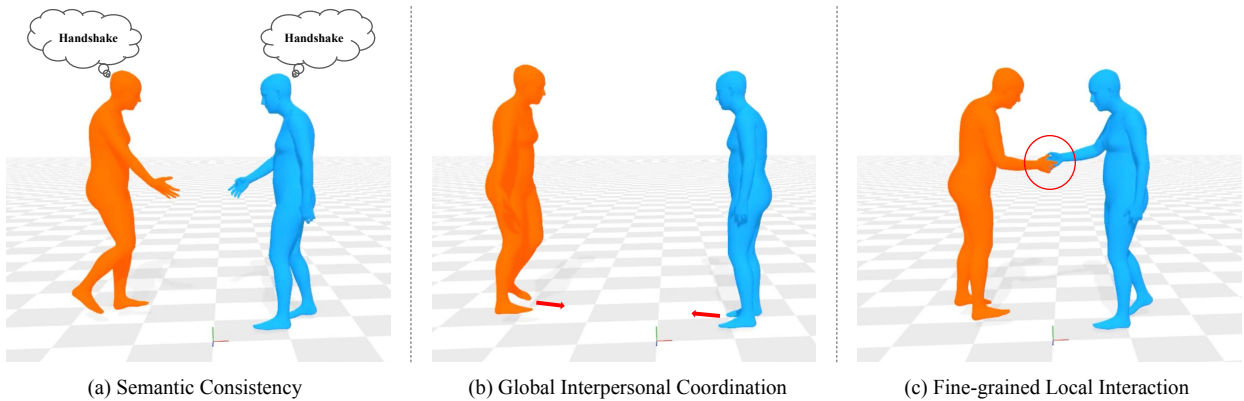


Fig. 3: Illustration of three major challenges in human-human interaction generation: (a) Semantic consistency; (b) Global interpersonal coordination; and (c) Fine-grained local interaction. All figures are adapted from [244].

without relying on extensive interaction datasets, instead leveraging the knowledge of human kinematics embedded in pre-trained LLMs through carefully designed prompts. LLMs can provide temporal specifications of interactions, identify relevant joint involvement, and describe precise interaction dynamics.

4 Human Interaction Motion Generation

This section elaborates on solutions for generating interactive human motions across four categories, as illustrated in Fig. 2: human-human interactions (Sec. 4.1), human-object interactions (Sec. 4.2), human-scene interactions (Sec. 4.3), and multi-entity interactions involving combinations of these elements (Sec. 4.4).

4.1 Human-Human Interaction Generation

Human-human interaction (HHI) research spans from dyadic interactions to group dynamics. For two-person interactions, the literature addresses two primary tasks: actor-reactor generation [60, 191], which synthesizes reactive motions in response to an actor’s movements, and synchronized interaction generation [91, 124], which simultaneously creates coordinated motions for both participants. Research also extends beyond dyadic interactions to group scenarios [52, 185], addressing the synthesis of coordinated movements among multiple participants.

Generating realistic HHI motions requires addressing three critical aspects, as illustrated in Fig. 3: semantic consistency, global interpersonal coordination, and fine-grained local interaction. Human interactions are inherently intention-driven. *Semantic consistency* ensures coherent and meaningful movements between participants that align with these intentions. For example, in social interactions like Fig. 3 (a), body movements

serve specific social gestures (e.g., handshakes), while in the duet dance, movements synchronize with musical cues. To enforce semantic consistency, existing approaches incorporate conditioning signals, such as textual descriptions or music. *Global interpersonal coordination* manages natural spatial relationships between interacting individuals (Fig. 3 (b)), including relative positions, mutual orientations, and interpersonal distances across scenarios. This coordination requires each person’s global position to be responsive to their partner’s movements, enabling fluid and harmonious interactions. *Fine-grained local interaction* addresses precise close-proximity interactions between body parts, such as hand-holding (Fig. 3 (c)) and hugging. This aspect focuses on encouraging realistic contact while minimizing artifacts like interpenetration between bodies. A comprehensive analysis of HHI generation methods is provided in Table 1.

4.1.1 Modeling Semantics of HHI

Human interactions encompass diverse semantic contexts across varying scenarios. This section reviews existing approaches for interaction generation based on their contextual constraints, including past interactions, partner motions, action categories, texts, and audio.

Conditioning on Past Interactions. Early research on HHI generation focused on predicting future interactive motions using past interaction motions. Kundu et al. [109] propose a motion generation architecture that alternates between two fixed-length cross-person motion prediction recurrent models to generate actor and reactor motions sequentially. This approach enables long-term motion synthesis while maintaining temporal synchronization within each window. Baruah and Banerjee [12] develop a predictive agent with two core

Table 1: Representative works of human-human interaction motion generation.

Method	Year	Venue	Model	Condition	Multi-Human Interaction Dataset	Single-Human Dataset
Shan et al. [185]	2024	ECCV	Diffusion	Text Description	LAION-Pose [185], WebVid-Motion [185], InterHuman [124]	HumanML3D [68]
FreeMotion [52]	2024	ECCV	Diffusion	Actor's Motion, Spatial Signal, Text	InterHuman [124]	-
ReMoS [60]	2024	ECCV	Diffusion	Actor's Motion	ReMoCap [60], ExPI [70], 2C [186], InterHuman [124]	-
ReGenNet [246]	2024	CVPR	Diffusion	Actor's Motion	NTU RGB+D 120 [127], InterHuman [124], Chi3D [54]	-
In2In [169]	2024	CVPRW	Diffusion	Text Description	InterHuman [124]	HumanML3D [68]
InterControl [235]	2024	NeurIPS	Diffusion	Spatial Signal, Text Description	-	HumanML3D [68], KIT-ML [168]
InterGen [124]	2024	IJCV	Diffusion	Text Description	InterHuman [124]	-
PriorMDM [184]	2024	ICLR	Diffusion	Text Description	3DPW [141]	HumanML3D [68], BABEL [172]
Duolando [191]	2024	ICLR	LLM	Actor's mMotion, Audio	DD100 [191]	-
Social Diffusion [206]	2023	ICCV	Diffusion	Past Motion	Haggling [96], MuPoTS-3D [144], 3DPW [141]	-
ActFormer [245]	2023	ICCV	GAN, Transformer	Action Class	NTU RGB+D 120 [127], GTA Combat [245]	BABEL [172]
InterFormer [32]	2023	TMM	Transformer	Actor's Motion	SBU Kinect [257], K3HI [84], DuetDance [109]	-
Tanaka and Fujiwara [203]	2023	ICCV	Transformer	Text Description	NTU RGB+D 120 [127]	-
DSAG [72]	2023	WACV	cVAE	Action Class, Past Motion	NTU RGB+D 120 [127]	HumanAct12 [69], UESTC [92], Human3.6M [90]
SoMoFormer [221]	2023	WACV	Transformer	Past Motion	3DPW [141], CMU-MoCap [113], MuPoTS-3D [144]	AMASS [139]
Guo et al. [70]	2022	CVPR	Transformer	Past Motion	ExPI [70]	-
MUGL [138]	2022	WACV	cVAE	Action Class, Past Motion	NTU RGB+D 120 [127]	-
Interaction Mix and Match [61]	2022	SCA	GAN	Action Class, Actor's Motion	SBU Kinect [257], 2C [186]	-
Men et al. [145]	2022	CAG	GAN	Actor's Motion	SBU Kinect [257], HHOI [189], 2C [186]	-
TRiPOD [4]	2021	ICCV	Graph, Regression	Past Motion, Video	3DPW [141]	-
MRT [226]	2021	NeurIPS	Transformer	Past Motion	3DPW [141], CMU-MoCap [113], MuPoTS-3D [144]	-
Baruah and Banerjee [12]	2020	CVPRW	Agent (Regression)	Past Motion	SBU Kinect [257], K3HI [84]	-
Yang et al. [253]	2020	SIGGRAPH	Graph	Audio	Private Dataset	-
Kundu et al. [109]	2020	WACV	Regression	Past Motion	DuetDance [109], CMU-MoCap [113], SBU Kinect [257]	-
Adeli et al. [3]	2020	RA-L	Regression	Past Motion, Video	NTU RGB+D 120 [127]	-
Joo et al. [96]	2019	CVPR	AE	Actor's Motion	Haggling [96]	-
Ahuja et al. [5]	2019	ICMI	Attention-Based	Actor's Motion, Audio	Private dataset	-
Christos Mousas [154]	2018	VR	Graph	Actor's Motion	CMU-MoCap [113]	-
Action-Reaction [87]	2014	ECCV	Graph	Video	UT-Interaction [181], SBU Kinect [257]	-

components: an observation module that dynamically identifies salient body parts from previous motions and encodes them as pose features, and a recurrent motion completion module that predicts subsequent poses. This architecture facilitates the generation of contextually appropriate interactive motions. MRT [226] introduces a multi-range transformer comprising local-range and global-range encoders. The local-range encoder extracts individual motion features, while the global-range encoder captures inter-person interaction features. This architecture ensures semantic consistency and scales to both dyadic and multi-person scenarios, supporting up to 15 individuals by decoupling local features from global interactions. Similarly, Guo et al. [70] and SoMoFormer [221] leverage transformer architectures for semantic consistency in motion generation. Guo et al. implement a cross-interaction attention module for bidirectional motion information exchange, while SoMoFormer employs learned identity embeddings to maintain semantic alignment between participants. Social Diffusion [206] adopts a recurrent diffusion model for simultaneous multi-person motion generation, incorporating an order-invariant averaging function to aggregate motion features while preserving social roles and interaction dynamics.

Conditioning on Partner Motions. Partner motion conditioning, also known as reactive motion synthesis, focuses on generating one person's motion in response to their partner's motion state. Christos Mousas [154] proposes a real-time HMM-based model for virtual dance partner generation. The model represents dance sequences as a graph of paired actor-reactor motion vectors, maintaining semantic alignment between roles. The HMM supports jump-state transitions to accommodate improvisation, enabling the virtual reactor to adapt dynamically to the actor's movements. Sebastian

et al. [197, 198] predict subsequent poses using a gated mixture of expert networks that processes phase features extracted from both the character and its opponent's current poses. Men et al. [145] develop a GAN-based approach, incorporating a temporal seq2seq attention module in the generator to preserve semantic consistency across key temporal steps. Building on this, InterFormer [32] implements a Transformer with temporal and spatial attention mechanisms, introducing a first-frame loss function to align initial poses. This alignment is particularly valuable given the limited availability of long-distance interaction training data. ReGenNet [246] adopts a diffusion model for iterative reactor motion generation, employing a simple yet effective strategy of concatenating actor motion features with generated reactor motion at each timestamp. ReMoS [60] extends this diffusion-based framework by incorporating spatio-temporal cross-attention and hand-interaction-aware cross-attention. These additions enable the model to analyze correlations between actor and reactor motion features, resulting in synchronized whole-body interactions with enhanced semantic consistency.

Conditioning on Action Categories. Action class labels provide a approach to encode high-level motion semantics. MUGL [138] and DSAG [72] implement deep learning encoder-decoder architectures based on conditional Gaussian Mixture VAE [46], where encoded features are modulated by action class labels to capture semantic relationships across participants' motions. ActFormer [245] employs a GAN-based Transformer framework that converts latent vector sequences and action labels into multi-person motion sequences. The model represents action classes as token embeddings combined with latent vectors, ensuring semantic consistency across generated motions. Interaction Mix and Match [61] advances reactive motion synthesis using a GAN with multi-hot class

embeddings, enabling the generation of reactor motions using single-class or designed class combinations.

Conditioning on Texts. Recent advances enable text-driven human interaction motion generation. Tanaka et al. [203] approach this task using a transformer model that encodes paired text prompts in active and passive voices for actor and reactor roles, effectively maintaining distinct semantic roles throughout asymmetric interactions. Several subsequent works [124, 169, 184, 235] adopt diffusion-based approaches with text conditioning.

PriorMDM [184] introduces a lightweight communication block to coordinate two frozen Motion Diffusion Models (MDMs) [210], widely used in text-to-motion generation, enabling two-person motion generation while preserving pre-trained model’s capabilities. Building on this, InterGen [124] incorporates CLIP-encoded text prompts and a mutual attention mechanism in two transformer-based denoisers with shared weights. This shared contextual understanding prevents mode collapse, where generated interactions may result in unrelated motion semantics between participants. In2IN [169] implements multi-head cross-attention modules within a transformer-based Siamese diffusion model for refined interaction control. The model employs a multi-weight CFG strategy that independently weights interaction and individual description influences, enabling precise control over movement diversity while maintaining semantic coherence. InterMask [91] takes a different approach, encoding two-person motions into 2D discrete token maps and using generative masked modeling for text-to-motion generation. Recent work has expanded beyond dyadic interactions to handle multi-person scenarios [52, 185]. Notably, Shan et al. [185] propose a unified transformer-based diffusion framework featuring interleaved pose and motion layers. Pose layers, conditioned on text embeddings, ensure semantic consistency, while motion layers, conditioned on individual poses, maintain temporal alignment between participants.

Conditioning on Audio. Interactive human motion can also be generated from audio signals, such as conversational speech and music. Unlike text conditioning, audio-driven generation requires precise temporal alignment. Ahuja et al. [5] introduce a dyadic residual attention model that combines two components: a monadic module processing only the reactor’s audio and motion, and a dyadic module integrating both participants’ audio, motion, and predicted reactor dynamics. This architecture generates responsive reactor movements that align with both actor motion and audio cues. Yang et al. [253] develop a motion graph incorporating audio-motion coordination features including phonemic clause

alignment, speaker hesitations, and listener responses. This approach enables the generation of synchronized multi-human motions that coherently follow conversational dynamics. Duolando [191] presents a GPT-based generative model to predict follower dance motions autoregressively, guided by both music and leader motion. The model processes audio features extracted via Librosa [143], mapping them to match motion feature dimensions. This design ensures balanced semantic alignment between musical and motion elements.

4.1.2 Maintaining Global Interpersonal Coordination

Maintaining accurate global spatial alignment and mutual orientation between interacting individuals is crucial for realistic interaction generation. Recent models have addressed this challenge through various approaches.

Several works focus on spatial guidance and loss functions. ReMoS [60] implements a spatial guidance function during inference to align reactor movements with actor positions, enhancing spatial coherence. ReGenNet [246] introduces a distance-based interaction loss that minimizes discrepancies in body poses, orientations, and translations. InterControl [235] extends MDM [210] by incorporating Motion ControlNet [263] to condition the model on spatial control signals, improving temporal alignment.

Other approaches emphasize representation and encoding strategies. InterGen [124] employs a non-canonical motion representation that encodes global joint positions and orientations in a unified world frame. SoMoFormer [221] integrates grid positioning embeddings to encode global locations, effectively capturing spatial relationships between participants. MUGL [138] and DSAG [72] implement global trajectory encoder-decoder modules with specialized loss functions to enforce movement path alignment.

Some models incorporate additional learning techniques. Duolando [191] utilizes off-policy reinforcement learning to improve the handling of novel leader motions, reducing unrealistic displacements and skating artifacts. Joo et al. [96] propose an autoencoder-based network for haggling scenarios that incorporates both body poses and face orientations to improve spatial alignment with ground truth.

4.1.3 Capturing Fine-Grained Local Interaction

Fine-grained local interactions, such as handshakes and face touching, require precise modeling of synchronized and complementary movements between proximate body parts of interacting individuals. Recent models have

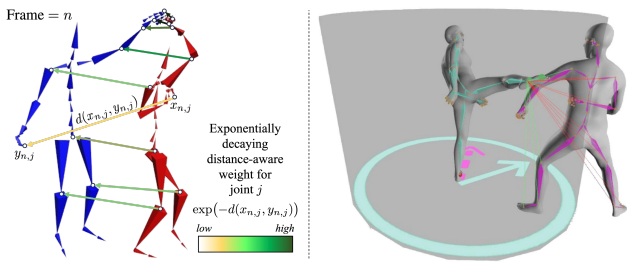


Fig. 4: Examples of distance-aware interaction mechanisms. (Left) ReMoS’s [60] Distance-Aware Reaction Loss applies an exponentially decaying function to prioritize reactor joints closer to the actor. (Right) InterGen [124] introduces Joint Distance Loss, which activates only when the horizontal distance between two individuals falls within a specified range, represented by the cylindrical region in the figure. Figures are adapted from [60, 124].

developed various strategies to enhance physical contact accuracy and interaction realism.

Several approaches focus on distance-based mechanisms. ReMoS [60] implements an exponentially decaying distance-aware reaction loss that prioritizes reactor joints closer to the actor, improving the fidelity of close-range interaction, as illustrated in Fig. 4 (Left). InterGen [124] employs a joint distance map loss that activates only within specific proximity thresholds, strengthening physical connections during interactions, as illustrated in Fig. 4 (Right). InterFormer [32] incorporates an interaction distance module that integrates softmax-scaled joint distances into the attention matrix, effectively modeling fine-grained interactions by weighting closer joints more heavily.

Architectural and strategy designs are addressed in other works. Duolando [191] utilizes a VQ-VAE to model relative joint translations between participants, enhancing the authenticity of physical contact. InterControl [235] guides motion generation using LLM-generated interaction descriptions that specify contact points and temporal progression.

4.2 Human-Object Interaction Generation

Human-object interaction (HOI) generation aims to synthesize realistic, context-aware motion sequences depicting humans engaging with 3D objects. This capability enhances system functionality and user immersion in robotics, virtual reality, human-computer interaction, and computer graphics applications.

Current research primarily addresses two key challenges: interaction semantic relevance, and spatial and physical constraints. *Interaction semantic relevance* ensures that generated motions authentically reflect interaction intents and proper object functionality—for example, ‘lifting’ a book or ‘sitting’ on a chair—while

maintaining plausibility and fidelity. *Spatial and physical constraints* take charge of adherence to physical laws and contact dynamics, requiring precise alignment between human body parts and object geometries while respecting gravity, friction, and biomechanical limits.

These challenges are being addressed through sophisticated data-driven models, advanced physics-based simulations, and multimodal data integration, establishing 3D HOI generation as a rapidly evolving field in computer vision and graphics. A comprehensive analysis of human-object interaction generation methods is presented in Table 2. This section reviews recent innovations in semantic relevance and constraint modeling.

4.2.1 Modeling Semantic of Human-Object Interaction

Early approaches like GOAL [200] and SAGA [238] focus on generating whole-body motions for object grasping, while IMoS [59] extends this by incorporating action categories to guide the grasping process. These approaches typically adopt a two-stage pipeline, wherein full-body motion is first synthesized using auto-regressive models or conditional variational autoencoders, followed by grasp motion optimization.

Recent works have leveraged diffusion models to generate human interactions with objects. Nifty [108] and COUCH [269] demonstrate this approach for human-furniture interactions. Many subsequent works utilize textual descriptions as conditioning signals. DiffH2O [33] introduces a two-stage diffusion process that decouples grasping and interaction phases while ensuring smooth transitions through grasp guidance. It employs a canonicalized hand-object representation incorporating distances between hand joints and their nearest points on the object mesh. Similarly, HOI-Diff [164] generates coarse-level human and object motions before estimating contact points through an affordance prediction diffusion model. GRIP [202] employs separate networks for arm denoising and body-hand motion consistency. HOIDiffusion [264] refines a controllable Stable Diffusion model using geometric structures from grasp trajectories, enabling precise pose control. Text2HOI [23] introduces a contact map prediction stage from canonical object meshes and text prompts, followed by denoising and refinement for accurate single-handed and dual-handed interactions. CHOIS [117] utilizes object geometry through Basis Point Set (BPS) representation [170] alongside language descriptions. HIMO-Gen [137] employs separate text-conditioned diffusion models for human and object motion, connected through a mutual interaction module. InterFusion [41] learns image-pose mappings to understand and generate various HOI scenes, while F-HOI [250] leverages multimodal large language

Table 2: Representative works of human-object interaction motion generation.

Method	Year	Venue	Model	Condition	Human-Object Interaction Dataset
DiffH2O [33]	2024	SIGGRAPH Asia	Diffusion	Text Description	GRAB [201]
InterDreamer [248]	2024	NeurIPS	LLM	Text Description	BEHAVE [13], CHAIRS [94]
CHOIS [117]	2024	ECCV	Diffusion	Text Description, Sparse Object Waypoints	OMOMO [118]
HIMO-Gen [137]	2024	ECCV	Diffusion	Text Description	HIMO [137]
InterFusion [41]	2024	ECCV	GPT-4V, Optimization	Text Description	ChatGPT prompts, DeepFloyd
F-HOI [250]	2024	ECCV	Multimodal LLM	Text Description	Semantic-HOI [250]
GraspDiff [287]	2024	TVCG	Diffusion	Object Shape	ObMan [81], HO3D [76], FPHAB [57]
HOIDiffusion [264]	2024	CVPR	Diffusion	Object Model, Text Description	DexYCB [26]
Text2HOI [23]	2024	CVPR	Diffusion	Text Description	GRAB [201], ARCTIC [53], H2O [112]
CG-HOI [45]	2024	CVPR	Diffusion	Text Description	BEHAVE [13], CHAIRS [94]
GEARS [283]	2024	CVPR	MLP, Attention	Hand-Object Trajectory, Object Shape	GRAB [201], InterCap [89], ObMan [81]
G-HOP [254]	2024	CVPR	Diffusion	Hand-Object Interaction Images, Object Mesh	ContactPose [16], DexYCB [26], YCB-Affordance [37], HO4D [132], GRAB [201], OakInk [251]
InterHandGen [116]	2024	CVPR	Diffusion	Hand Pose, Object Shape (Optional)	ARCTIC [53], InterHand2.6M [153]
NIFTY [108]	2024	CVPR	Diffusion	Initial Body Pose, Object Shape	BEHAVE [13]
IM-HOI [274]	2024	CVPR	Diffusion	IMU Recording, Monocular RGB Video	IMHD2 [274], BEHAVE [13], InterCap [89], CHAIRS [94], HODome [260]
GeneOHDiffusion [131]	2024	ICLR	Diffusion	Noisy Hand-Object Poses	GRAB [201], HO4D [132], ARCTIC [53]
ArtiGrasp [258]	2024	3DV	RL, Physics Simulation	Hand Pose Reference	ARCTIC [53]
GRIP [202]	2024	3DV	RNN	Body Pose, Object Motion	GRAB [201], InterCap [89], MoGaze [107]
MACS [188]	2024	3DV	Diffusion	Action Label, Object Mass	ManipNet Data [259]
PhysFullbody [17]	2024	3DV	RL	Hand-Object Reference Pose, Wrist Trajectory	GRAB [201]
TOHO [120]	2024	WACV	cVAE	Task Instructions	GRAB [201]
CWG-Grasp [162]	2024	-	cVAE, Optimization	Object Mesh	ReplicaGrasp [207], GRAB [201], CIRCLE [8]
GraspDiffusion [111]	2024	-	Diffusion	Object Mesh and Position	GRAB [201], BEHAVE [13], DexYCB [26], HICO-DET [25], V-COCO [73]
HOI-Diff [164]	2023	-	Diffusion	Text Description	BEHAVE [13], OMOMO [118]
OMOMO [118]	2023	SIGGRAPH Asia	Diffusion	Object Motions	OMOMO [118]
InterDiff [247]	2023	ICCV	Diffusion	Initial Pose	BEHAVE [13]
Chen et al. [28]	2023	SIGGRAPH	cVAE, Optimization	Object Shape	YCB [19]
CAMS [278]	2023	CVPR	cVAE	Init. Hand Pose, Object Goal Sequence, Object Shape	HO4D [132]
FLEX [207]	2023	CVPR	MLP	Object Shape	GRAB [201], ReplicaGrasp [207]
NeuralDome [260]	2023	CVPR	Neural Rendering	Multi-View Video Sequence	HODome [260]
SAGA [238]	2022	ECCV	cVAE	Human-Object Initial Pose, Object Shape	GRAB [201], HO3D [76], AMASS [139]
TOCH [282]	2022	ECCV	GRU	Hand-Object Image / Hand-Object Mesh	GRAB [201], HO3D [76]
DGrasp [54]	2022	CVPR	RL, Physics Simulation	Grasp Label (Image), Object Pose	DexYCB [26], HO3D [76]
GOAL [206]	2022	CVPR	cVAE, Optimization	Human-Object Initial Pose, Object Shape	GRAB [201]
IMoS [59]	2022	Eurographics	cVAE, Optimization	Action Labels, Object	GRAB [201]
GraviCap [39]	2021	ICCV	Regression, Optimization	Monocular RGB Videos	Gravicap Dataset
ManipNet [259]	2021	SIGGRAPH	RNN	Object Shape, Wrist-Object Trajectories	Object Manipulation Dataset
GrabNet [201]	2020	ECCV	cVAE, RNN	Object Shape	GRAB [201]
GanHand [37]	2020	CVPR	RNN	Single RGB Image	ObMan [81], YCB-Affordance [37]

models for fine-grained HOI generation tasks. InterDreamer [248] achieves zero-shot text-conditioned generation by using LLMs for high-level task planning.

A distinct category of methods focuses on object-guided interaction synthesis. OMOMO [118] generates full-body manipulation behaviors solely from object geometries and motions. TOHO [120] estimates object end positions from task descriptions which then guides the generation of human pose sequences. GraspDiffusion [111] employs a two-stage pipeline for synthesizing whole-body interactions given object mesh and its position information.

4.2.2 Spatial and Physical Constraints

Physical plausibility through accurate contact modeling is fundamental in HOI motion synthesis. Recent approaches have addressed this challenge through various contact-aware methodologies. This subsection also extends the discussion to encompass HOI pose generation for a comprehensive review.

Contact-guided methods focus on optimizing the spatial relationships between hands and objects through contact points or regions. CHOIS [117] and DiffH2O [33] implement contact guidance functions to minimize gaps and penetrations between the hand and the object meshes. Similarly, GraspDiff [287], GRIP [202], and GrabNet [201] employ refinement networks utilizing Chamfer distance [237] and proximity sensors to enhance grasp quality. In the realm of contact optimization, ContactOpt [65] predicts contact points and optimizes hand poses to achieve desired contact configurations, while ContactGrasp [15] introduces an optimization



Fig. 5: InterDiff [247] applies coordinate transformations to represent object states relative to contact points, resulting in simpler motion patterns (right column) compared to using absolute positions (middle column). Figures are adapted from [247].

framework that leverages attractive and repulsive values assigned to object surface points. ContactGen [128] advances these approaches by utilizing object-centric contact maps combined with *part maps* and *direction maps* to precisely locate hand contact points. RegionGrasp [230] aims to generate hand grasp poses with the thumb finger contacting specific regions of the object. Recent diffusion-based methods such as HOI-Diff [164] and CG-HOI [45] implement HOI affordance guidance during the sampling process to achieve coherent interaction synthesis. InterDiff [247] suggests that object motion relative to contact points on the human body

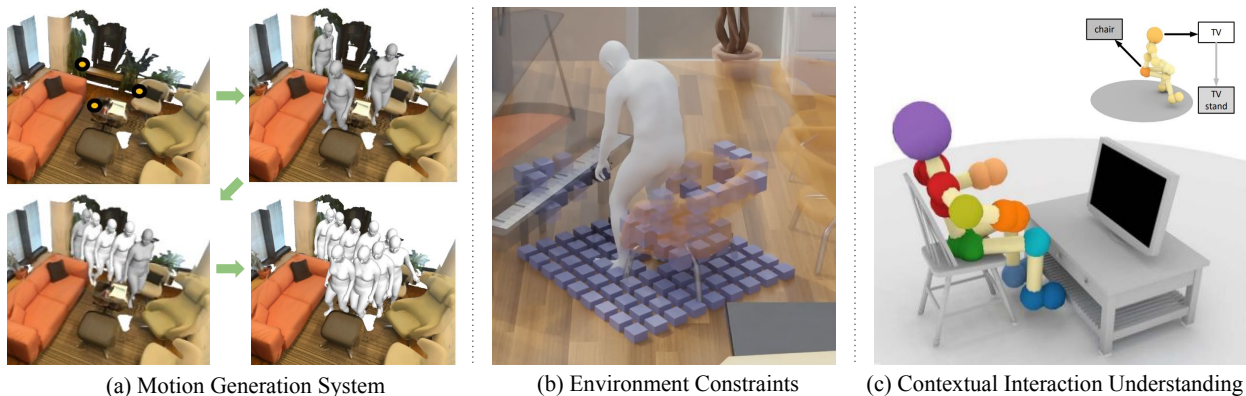


Fig. 6: Existing works model human scene interactions in three major aspects: (a) *Motion generation system* that decompose complex interactions into modular subtasks for systematic processing; (b) *Environment constraint models* that incorporate physical constraints between humans and their surroundings; and (c) *Contextual interaction understanding* that analyzes spatial relationships within the environment. Figures are adapted from [93, 182, 227].

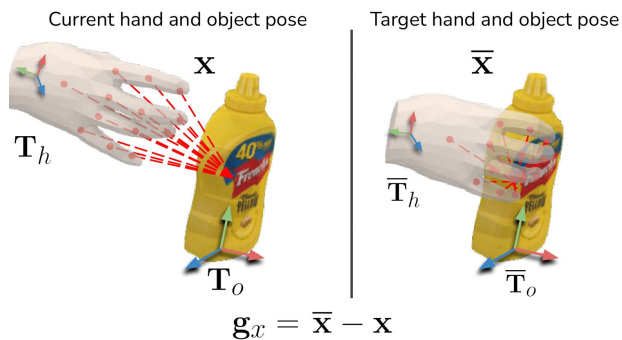


Fig. 7: Grasp [34] introduces the target distance component g_x which computes the displacement between current and target 3D joint positions relative to the object’s origin. Figures are adapted from [34].

shows simpler learnable patterns than its absolute positions, as illustrated in Fig. 5. In addition, DGrasp [34] incorporates the target distance as an input feature, promoting grasping at contact points proximal to those specified in the grasp reference data, as illustrated in Fig. 7.

Physics-based approaches have significantly improved interaction realism through simulation and learning. PhysFullbody [17] achieves full-body dexterous grasping through reinforcement learning in a physics simulation. ManipNet [259] demonstrates fine-grained synchronization through learned contact constraints, while DGrasp [34] implements a PD-controller in a physics simulation to compute hand torques for precise object manipulation. Extending these capabilities, ArtiGrasp [258] synthesizes physically plausible bimanual grasping through reinforcement learning.

In addition, several innovative approaches have emerged for specialized interaction scenarios. NIFTY [108] develops neural interaction fields attached to objects, guiding an object-conditioned

human motion diffusion model to generate plausible contacts for diverse actions. GraspingField [100] employs an implicit representation by encoding grasps in a signed distance field, enabling 3D hand-object grasp reconstruction from single images. For specific manipulation tasks, Chen et al. [28] focus on nonprehensile pre-grasp motions by optimizing thumb and index finger contact trajectories. GEARS [283] introduces a novel joint-centered point-based geometry sensor combined with spatiotemporal self-attention to model joint correlations effectively. G-HOP [254] advances the field by utilizing interaction grids with diffusion-based generative priors. Most recently, GeneOHDiffusion [131] proposes a contact-centric HOI representation that parameterizes interactions in a region-specific coordinate system, significantly enhancing generalization across diverse interaction scenarios.

4.3 Human-Scene Interaction Generation

In everyday life, humans effortlessly navigate and interact with complex environments. Recreating this natural ability is essential for 3D applications such as gaming, simulation, and character animation in virtual environments. Human-scene interaction (HSI) entails modeling how humans move and interact with their surroundings while adhering to a set of physical rules, such as collision avoidance and aligning with semantic or contextual constraints. Additionally, supplementary signals—such as text prompts, action labels, and target goals—further enhance the control and precision of motion generation in these systems.

Existing work attempts to achieve scene-aware motion generation through these three pillars: motion generation systems, environment constraints, and contextual interaction understanding, as illustrated in Fig. 6. *Mo-*

Table 3: Representative works of human-scene interaction motion generation.

Method	Year	Venue	Model	Condition	Human-Scene Interaction Dataset	Other Human Dataset
CLoSD [208]	2025	ICLR	RL, Physics Simulation	Text Description	-	AMASS [139]
GHOST [148]	2025	WACV	cVAE	Text Description	HUMANISE [234]	-
LINGO [93]	2024	TOG	Diffusion	Text Description	LINGO [93]	-
UniHSI [240]	2024	ICLR	RL, Physics Simulation	Text Description	ScenePlan [240]	-
TeSMo [255]	2024	ECCV	Diffusion	Text Description	Loco-3DFRONT [255], SAMP [78]	HumanML3D [68]
MOB [130]	2024	ECCV	cVAE	Past Motion, Target Pose/Traj.	CIRCLE [8]	HumanML3D [68]
Xing et al. [242]	2024	ECCV	Graph Convolutional Network	Past Motion	GTA-IM [21], PROX [79], HUMANISE [234], GIMO [280]	-
AffordMotion [233]	2024	CVPR	Diffusion	Text Description	HUMANISE [234]	HumanML3D [68]
Cen et al. [22]	2024	CVPR	Diffusion	Text Description	HUMANISE [234]	-
GenZI [119]	2024	CVPR	Optimization	Text Description	-	-
Lou et al. [135]	2024	CVPR	cVAE	Past Motion, Gaze	GTA-IM [21], GIMO [280]	-
S2Fusion [204]	2024	CVPR	Diffusion	Sparse Tracking Signals	CIRCLE [8], GIMO [280]	-
TRUMANS [95]	2024	CVPR	Diffusion	Action class	TRUMANS [95]	-
InterScene [160]	2024	3DV	RL, Physics Simulation	Object-Level Action Class	SAMP [78]	-
Purposer [215]	2024	3DV	cVAE	Past Motion, Target Pose/Traj.	HUMANISE [234]	BABEL [172]
MCLD [56]	2024	IEEE TIP	Diffusion	Past Motion	GTA-IM [21], PROX [79]	-
SIMS [229]	2024	-	RL, Physics Simulation	Text Script	CIRCLE [8], SAMP [78]	100Style [142]
DIP [62]	2024	-	Diffusion	Text Description	-	BABEL [172], HumanML3D [68]
GPT-Connect [174]	2024	-	Diffusion	Text Description	HUMANISE [234]	-
LaserHuman [36]	2024	-	Diffusion	Text Description	LaserHuman [36]	-
PAAK [155]	2023	WACV	Optimization	-	PROX [79]	-
DIMOS [277]	2023	ICCV	RL	Target Pose	SAMP [78]	AMASS [139]
LAMA [115]	2023	ICCV	RL	Interaction Cue	-	Self-Captured
Narrator [249]	2023	ICCV	cVAE	Text Description	PROX [79]	-
MAMMOS [125]	2023	ICCVW	cVAE	Action Class	PROX [79]	-
Hassan et al. [80]	2023	SIGGRAPH	RL, Physics Simulation	Tasks	SAMP [78]	-
CIRCLE [8]	2023	CVPR	Transformer	Goal Position	CIRCLE [8]	-
SceneDiffuser [88]	2023	CVPR	Diffusion	-	PROX-S [276], LEMO [267]	-
Mir et al. [151]	2023	3DV	Transformer	Action Keypoints	-	AMASS [139]
HUMANISE [234]	2022	NeurIPS	cVAE	Text Description	HUMANISE [234]	-
COINS [276]	2022	ECCV	cVAE	Object-Level Action Class	PROX-S [276]	-
GAMMA [272]	2022	CVPR	cVAE	Past Motion, Goal	-	AMASS [139]
Wang et al. [225]	2022	CVPR	cVAE	Target Actions	PROX [79]	-
SAMP [78]	2021	ICCV	cVAE	Target Goal	SAMP [78]	-
Wang et al. [227]	2021	CVPR	cVAE	Body Sub-Goals	PROX [79]	-
Cao et al. [21]	2020	ECCV	cVAE	Past Motion	GTA-IM [21]	-
PSI [271]	2020	CVPR	cVAE	-	PROX [79]	-
PLACE [268]	2020	3DV	cVAE, Optimization	-	PROX [79]	-
Neural State Machine [196]	2019	TOG	RL	Goal Action	-	Self-Captured
3DAffordance [122]	2019	CVPR	GAN, Optimization	Scene Image	-	-
PiGraphs [182]	2016	TOG	Interaction Graph	Object Relationships	PiGraphs [182]	-

tion generation system decomposes the complex scene-aware motion synthesis into modular and more tractable subtasks, a common strategy in recent researches. *Environment constraints* ensure physical plausibility by maintaining coherence between generated motions and spatial constraints. These constraints align human poses and movements with scene geometry and surfaces, preserving natural motion dynamics and physical consistency throughout the interaction sequence. *Contextual interaction understanding* enhances system capabilities through semantic comprehension of environmental context, enabling meaningful and nuanced interactions. This encompasses graph-based modeling of object relationships for joint-level interactions, high-level planning through LLMs, and interpretation of scene affordances via image-based cues.

These three aspects are fundamental to generating lifelike, physically coherent, and semantically appropriate human motions in 3D scenes, forming the foundation for contemporary advances in scene-aware motion generation. We summarize the characteristics of human-scene interaction generation methods in Table 3. The following sections explore recent advancements in addressing these challenges within scene-aware motion generation.

4.3.1 Building Motion Generation System

Several methods adopt hierarchical or stage-wise pipelines to synthesize interactions with the scene. COINS [276] first generates a plausible human pelvis

pose and then completes the body pose for static human-scene interaction. Wang et al. [227] propose a framework for synthesizing long-term motion by generating static sub-goal poses from given root information and connecting them with a short-term motion completion module. SAMP [78] first predicts an oriented goal location for interaction, then generates a collision-free path, and finally predicts the full-body motion required to reach the target. Wang et al. [225] first synthesize human-scene interaction anchors based on action labels, then complete motions by integrating these anchors with planned paths. PAAK [155] proposes a method for placing existing human animations into scenes by identifying keyframes that are most critical for interactions with the scene and using them to accurately position the animation within the environment. MAMMOS [125] synthesizes interaction anchors for each individual character and completes motions by integrating timelines to account for multi-human interactions. Mir et al. [151] first infer static key poses from action keypoints defined by users and then complete a variety of motion types—such as transitions in/out and walking—utilizing a goal-centric canonical coordinate space to complete motion sequences. TeSMo [255] synthesizes navigation motion based on the generated root trajectory and subsequently produces interaction motion with the target object. DIP [62] decomposes the entire command task into a list of subtasks and identifies corresponding keyframes. Then it completes motions conditioned on actions and

keyframe joints, which are subsequently refined through time-variant blending.

The auto-regressive motion generation strategy enables the generation of arbitrarily long sequences, and several methods adopt this approach. MOB [130] formulates an auto-regressive motion controller by utilizing historical motion states and integrating target positions or trajectories, demonstrating its capability to produce motion in both static and dynamically changing scenes. MCLD [56] predicts future human motion from past body movements using a conditional diffusion formulation. TRUMANS [95] and LINGO [93] employ an auto-regressive diffusion sampling approach to enable the progressive generation of long motion sequences. They replace the preceding segment of frames with the previous corresponding last segment and then generate continuous motion from these.

Another line of work formulates motion generation as a Markov decision process and utilizes reinforcement learning (RL) based frameworks to generate continuous motion sequences. GAMMA [272] uses a policy network to explore latent representations for marker prediction and applies a tree-based search to find motion primitives. DIMOS [277] creates static human-scene interaction poses for sub-goals and uses a policy network to generate scene-conditioned latent actions, which are later converted into motion primitives by a pre-trained model. LAMA [115] derives action signals from a motion controller, transforms them into motion features, and identifies motion segments using motion-matching algorithms. These motion sequences are further optimized within a learned manifold for scene manipulation. Additionally, physics simulators, such as [140], have been applied to this formulation. Hassan et al. [80] train a policy and motion discriminator to achieve goal-based interactions with the scene and generate natural motion consistent with the dataset. UniHSI [240] transforms language commands into an ordered condition for interaction, referred to as the Chain of Contacts (CoC), and designs a robust unified controller for executing various interaction tasks. InterScene [160] employs a finite-state machine to coordinate navigation and interaction controllers, enabling long-term interactions within a scene. SIMS [229] combines high-level LLM planning with low-level physical control by extracting interactions from real videos into short scripts, which are then combined into long-term narratives. The system matches these narratives with suitable scene layouts using graph-based methods and also applies a finite-state machine to translate scene information into physical control policies for practical execution.

4.3.2 Capturing Environment Constraints

A key challenge in scene-aware motion generation is maintaining adherence to spatial constraints and physical rules. One approach uses post-optimization or physics simulation techniques to refine the generated motion, ensuring that it aligns with these constraints and rules. PSI [271] refines the static body results to encourage contact and prevent interpenetration between the body and the scene. COINS [276] refines the static pose results to enhance physical plausibility by aligning predicted contact regions with objects according to the specified actions. Wang et al. [227] leverage a cVAE to generate initial static poses conditioned on 3D scenes. After generating the full motion sequence from anchors, they refine the resulting motions through post-optimization, mitigating collisions and enhancing contact at body vertices, as well as motion smoothness and foot constraint. Wang et al. [225] introduce Neural Mapper to generate diverse, obstacle-free paths that extend conventional path-finding algorithms. Building upon a path, they complete motion and further optimize it by utilizing a physical loss. Narrator [249] introduces an Interaction Bisector Surface (IBS) loss to effectively handle penetration and contact issues during scene-aware optimization. CLoSD [208] enhances physical plausibility by incorporating a physics simulator after diffusion-based generation.

Another approach focuses on effectively modeling spatial constraints during the process of motion generation. These methods can be categorized based on their key technical contributions: First, several works focus on encoding scene-body relationships through specific feature representation. PLACE [268] explicitly models body-environment proximity using BPS [170] within a cVAE architecture. MOB [130] learns motion-scene relationships through a canonicalized space occupancy grid, training exclusively on human-only motion data. AffordMotion [233] introduces an affordance map based on skeleton-scene distance fields, generating motions from language instructions via this intermediate representation. S2Fusion [204] combines PointNet-extracted scene features with periodic tracking signals. Xing et al. [242] propose a mutual distance representation incorporating per-vertex signed distances and per-basis point distances. TRUMANS [95] conditions a diffusion model on local occupancy voxels centered on the pelvis, encoded via ViT [47]. On top of this, a few other works focus on novel architectural designs and learning strategies. CIRCLE [8] employs a transformer-based refinement module utilizing scene geometry features from BPS or PointNet [173], derived from initial body surfaces. SceneDiffuser [88] incorporates a cross-attention module for

Table 4: Representative works of human-mix interaction motion generation. (HH: Human-Human, HO: Human-Object, HS: Human-Scene.)

Method	Year	Venue	Tasks	Model	Condition	Dataset
Sitcom-Crafter [27]	2025	ICLR	HH, HS	Diffusion	Scene, Text Description	InterHuman [124], Inter-X [244]
HOI-M ³ [261]	2024	CVPR	HH, HO	Diffusion	Object	HOI-M ³ [261]
Shu et al. [189]	2016	IJCAI	HH, HO	Graph	Past Motion, Object	HHOI [189]

scene point cloud encoding and integrates physics-based objectives during sampling to ensure proper contact and collision avoidance. DIP [62] enhances the diffusion process with implicit policy optimization, guided by contact and non-penetration rewards. Lou et al. [135] extract both local and global salient points for detailed spatial understanding and trajectory planning, integrated through scene-aware cross-modal attention. LINGO [93] employs dual voxels for current and predictive contexts, with adaptive positioning based on motion stage and interaction targets.

4.3.3 Understanding Spatial Interaction Context

An advanced understanding of the spatial layout and relationships in the scene is also important for HSI generation. This information would navigate the character in the scene and direct the interactions with specific scene entities.

PiGraphs [182] learns a probabilistic graph of human-centric interaction, where nodes represent objects and body parts, and edges encode the spatial relationships between interacting joints and objects. Purposer [215] proposes a method for estimating dense body-to-scene contact using vertex-level semantic labels, enabling the semantically appropriate placement of posed humans in 3D scenes. Neural State Machine [196] extracts extensive motion features regarding its surrounding cylinder environment, and employs a gated network and a motion prediction network that processes the current state and the goal action vector to predict posture and control variables for sequential frames. COINS [276] synthesizes static human-scene interactions derived from ‘action-object’ semantics, and combines atomic interactions into compositional interactions. Narrator [249] employs a *joint global and local scene graph* for spatial relationship modeling and a *part-level action* mechanism to align body parts with actions for realistic and text-faithful interactions.

Recent advances in text-conditioned scene-aware motion generation have leveraged both semantic understanding and large language models (LLMs). GHOST [148] enhances motion synthesis by learning a shared text-scene feature space that improves semantic scene understanding. GPT-Connect [174] utilizes LLMs to comprehend scene context and generate in-

formative human skeleton configurations, which subsequently guide the motion diffusion model’s output. Taking a unified approach, UniHSI [240] formulates human-scene interaction through sequential transitions of joint-object contact pairs, employing an LLM planner to transform language commands into structured task plans. Building on this trajectory, Cen et al. [22] integrate scene graph construction with LLM-based textual analysis to identify target objects and synthesize contextually appropriate interaction motions.

Another line of work utilizes image information to guide the motion generation process. 3DAffordance [122] generates semantically plausible poses on scene images and maps human poses into scene voxels. Cao et al. [21] predict human motion influenced by the scene using a single-scene image and 2D pose histories as input. GenZI [119] synthesizes 2D human interactions in image space using Vision-Language Models (VLMs) with a textured 3D scene across multiple views, lifting them to 3D through a robust optimization process for human parameters.

4.4 Human-Mix Interaction Generation

Recent research has expanded to address more complex environments involving multiple entities—objects, scenes, and other humans—in interactive motion synthesis. We summarize the characteristics of human-mix interaction generation methods in Table 4.

Shu et al. [189] pioneer the exploration of human-human-object interactions by reducing the problem complexity through object trajectory abstraction. By treating objects as additional joints, their approach leverages graph models to predict interactive human motions, enabling simultaneous modeling of human-human and human-object close interactions. HOI-M3 [261] advances this framework by unifying multi-human information and multi-object poses into a comprehensive motion embedding. The system employs PointNet [173] for extracting geometric object features and utilizes a diffusion model with concatenated object and motion embeddings to generate semantically coherent interactive motions for both humans and objects.

Sitcom-Crafter [27] addresses the challenge of generating expressive human-human interactions within 3D scenes. Acknowledging the scarcity of datasets that

Table 5: **Human-human interaction datasets.** This table summarizes key statistics and features of various human-human interaction datasets. Subjects: The number of individuals involved in the dataset; Sequences: The number of motion clips available; Frames: The total number of frames capturing 3D human motions; Length: The cumulative duration of the dataset’s motion data (in hours); Acquisition: The method used to obtain motion data (e.g., multi-view RGB videos denoted as “mRGB”); Modality: The representation format of motion data; Video, Text, Audio: Indicates whether the dataset includes corresponding modalities.

Dataset	Year	Venue	Subjects	Sequences	Frames	Length	Acquisition	Modality	Video	Text	Audio
Inter-X [244]	2024	CVPR	89	11,388	8.1M	-	MoCap	SMPL-X	✓	✓	✓
InterHuman [124]	2024	IJCV	60	7,779	107M	6.56h	mRGB	SMPL	✓	✓	✓
ReMoCap [60]	2024	ECCV	9	-	275.7K	2.04h	mRGB	3D Skeleton	✓	✓	✓
LAION-Pose (image-only) [185]	2024	ECCV	-	-	8M	-	sRGB	SMPL	✓	✓	✓
WebVid-Motion [185]	2024	ECCV	-	3,500	-	-	sRGB	SMPL	✓	✓	✓
DD100 [191]	2024	ICLR	10	100	210K	1.95h	MoCap	SMPL-X	✓	✓	✓
Hi4D [256]	2023	CVPR	40	100	11K	-	mRGB	SMPL	✓	✓	✓
GTA Combat [245]	2023	ICCV	14	6,900	-	-	MoCap (GTA-V)	3D Skeleton	✓	✓	✓
ExPI [70]	2022	CVPR	4	115	30K	0.33h	MoCap + mRGB	3D Skeleton + 3D Mesh	✓	✓	✓
MultiHuman [279]	2021	ICCV	278	150	-	-	mRGB	SMPL-X	✓	✓	✓
Chi3D [54]	2020	CVPR	6	631	486K	2.70h	MoCap + mRGB	GHUM + SMPL-X	✓	✓	✓
You2Me [158]	2020	CVPR	10	42	77K	1.4h	mRGB-D	3D Skeleton	✓	✓	✓
2C [186]	2020	TVCG	2	8	-	0.06h	MoCap	3D Skeleton	✓	✓	✓
DuetDance [109]	2020	WACV	-	-	196K	1.09h	-	-	✓	-	-
NTU RGB+D 120 (interactive) [127]	2019	TPAMI	106	20,579	-	18.6h	RGB-D	3D Skeleton	✓	✓	✓
Talking With Hands 16.2M [114]	2019	ICCV	50	200	16.2M	50h	MoCap	3D Skeleton	✓	✓	✓
Haggling [96]	2019	CVPR	102	34	-	6h	mRGB-D	3D Skeleton	✓	✓	✓
MuPoTS-3D [144]	2018	3DV	8	20	8K	-	mRGB	3D Skeleton	✓	✓	✓
3DPW [141]	2018	ECCV	18	60	51K	-	sRGB + IMU	SMPL	✓	✓	✓
JTA [51]	2018	ECCV	10,800	512	461K	4.27h	MoCap (GTA-V)	3D Skeleton	✓	✓	✓
CMU-Panoptic [97]	2017	TPAMI	-	65	1.5M	5.5h	mRGB-D	3D Skeleton	✓	✓	✓
ShakeFive2 [58]	2016	HBV	10	153	34K	0.32h	RGB-D	3D Skeleton	✓	✓	✓
MARCOmI [49]	2015	CVPR	10	12	6.2K	0.07h	mRGB	3D Skeleton	✓	✓	✓
K3HI [84]	2013	Math. Probl. Eng.	15	320	8K	-	RGB-D	3D Skeleton	✓	✓	✓
SBU Kinect [257]	2012	CVPRW	-	300	7.5K	0.13h	RGB-D	3D Skeleton	✓	✓	✓
UMPM [1]	2011	ICCVW	30	36	400K	2.22h	MoCap + mRGB	3D Skeleton	✓	✓	✓
MHHI [133]	2011	CVPR	5	7	1.5K	0.01h	MoCap + mRGB	3D Skeleton + 3D Mesh	✓	✓	✓
UT-Interaction [181]	2010	ICPR	15	20	36K	0.33h	sRGB	No Skeleton	✓	✓	✓
CMU Graphics Lab MoCap (interactive) [113]	2008	-	6	53	7.6K	0.07h	MoCap + sRGB	3D Skeleton	✓	✓	✓

combine human-human interactions with 3D scene information, the authors propose an innovative solution: synthesizing implicit 3D Signed Distance Function points to simulate spatial obstacles. This synthetic training data enables effective collision avoidance while preserving motion fidelity.

5 Datasets

Over recent decades, researchers have developed multiple datasets for human interaction motion generation research. In this section, we present a comprehensive analysis of widely adopted datasets across four primary interaction categories: human-human (Table 5), human-object (Table 6), human-scene (Table 7), and human-mix (Table 8) interactions.

5.1 Human-Human Interaction Datasets

We review existing HHI motion datasets based on their distinct representations and conditioning modalities. Table 5 provides detailed statistics of current HHI datasets.

Human Skeleton Based Datasets. These datasets primarily represent human interactions through 3D skeletal data, capturing joint coordinates and body keypoints at sequential frames. Early contributions in this domain include CMU Graphics Lab MoCap [113], UPM [1],

SBU Kinect [257], K3HI [84], MARCOmI [49], ShakeFive2 [58], MuPoTS-3D [144], and 2C [186]. These pioneering datasets employ single RGB-D or multi-camera setups to capture multi-human interactions, providing sparse representations of human motion. More recent datasets have significantly expanded in scope, encompassing larger subject pools, longer action sequences, and more diverse social interactions. The NTU RGB+D 120 [127] dataset stands as a prominent example, featuring over 20,000 diverse motion sequences that have made it a standard benchmark in the field. Specialized datasets have also emerged, such as ReMoCap [60], which focuses on specific interaction contexts like dance and martial arts, providing two hours of dedicated human interaction data. In addition, innovative data acquisition methods have been purposed. You2Me [158] utilizes wearable devices to capture reactor motions from the actor’s perspective, establishing an innovative methodology for interaction data acquisition. Taking advantage of gaming technology, GTA Combat [245] and JTA [51] leverage the GTA-V engine to generate large-scale, visually consistent multi-person scenarios featuring diverse human poses and versatile multi-human interactions.

Human Shape Based Datasets. Beyond 3D skeleton data, several datasets incorporate 3D body mesh information, enabling high-fidelity modeling of human-human interactions through more comprehensive body structure representation. Datasets like 3DPW [141], Chi3D [54],

Table 6: Human-object interaction datasets. This table summarizes key statistics and features of various human-object interaction datasets. Subjects: The number of individuals involved in the dataset; Sequences: The number of motion clips available; Frames: The total number of frames capturing 3D human motions; Length: The cumulative duration of the dataset’s motion data (in hours); Acquisition: The method used to obtain motion data (e.g., multi-view RGB videos denoted as “mRGB”); Modality: The representation format of motion data; Images, Text: Indicates whether the dataset includes corresponding modalities.

Dataset	Year	Venue	Subjects	Object Types	Sequences	Frames	Length	Acquisition	Modality	Images	Text
HIMO [137]	2024	ECCV	34	53 Household Objects	3,376	4.08M	9.44h	MoCap	SMPL-X	✓	✓
Semantic-HOI [250]	2024	ECCV	-	-	-	20.4K	-	Existing Datasets + GPT-4V	SMPL-X	✓	✓
IMHD2 [274]	2024	CVPR	15	10 Everyday Objects	295	892K	-	mRGB + IMU Sensor	SMPL-H	✓	✓
OMOMO [118]	2023	TOG	17	15	-	-	-	mRGB	SMPL-X	✓	✓
CHAIRS [94]	2023	ICCV	46	81 Sittable Objects	1,390	1.8M	17.3h	mRGB + MoCap	SMPL-X	✓	✓
ARCTIC [53]	2023	CVPR	10	11 Articulated Objects	339	2.1M	1.2h	mRGB + MoCap	SMPL-X	✓	✓
HODome [260]	2023	CVPR	10	23	274	71M	4.5h	mRGB	SMPL	✓	✓
BEHAVE [13]	2022	CVPR	8	20 Common Objects	321	15.2K	4.2h	mRGB-D	SMPL	✓	✓
HOI4D [132]	2022	CVPR	-	-	-	-	-	-	-	✓	✓
H2O3D [77]	2022	CVPR	5	10	-	75K	-	mRGB-D	MANO	✓	✓
COUCH [269]	2022	ECCV	6	3 Chairs	500	648K	3h	MoCap	SMPL	✓	✓
InterCap [89]	2022	GCPR	10	10 Everyday Objects	223	67.3K	-	mRGB	SMPL-X	✓	✓
GRAVICAP [39]	2021	ICCV	4	4 Different balls	9	-	-	mRGB + MoCap	3D Skeleton	✓	✓
H2O [112]	2021	ICCV	4	-	-	571K	-	mRGB-D	MANO	✓	✓
DexYCB [26]	2021	CVPR	10	20	1000	582K	-	mRGB-D	3D Keypoints	✓	✓
GRAB [201]	2020	ECCV	10	51 Small Objects	1334	1.6M	3.8h	MoCap	SMPL-X	✓	✓
ContactPose [16]	2020	ECCV	50	25	-	-	-	mRGB-D	MANO	✓	✓
HO-3D [76]	2020	CVPR	10	10	68	77.5K	-	RGB-D	MANO	✓	✓
ObMan [81]	2019	CVPR	20	8 Everyday Objects	-	21K	-	GraspIt	SMPL-H	✓	✓
ContactDB [14]	2019	CVPR	50	50 Household Objects	-	375K	-	mRGB-D	3D Mesh	✓	✓
Dexter+Object [194]	2016	ECCV	2	2 Cuboids	6	3K	-	RGB-D	2D Keypoints	✓	✓

MultiHuman [279], and Hi4D [256] utilize parametric body models, such as SMPL [163], SMPL-X [134], and GHUM [243], to capture subtle variations in full-body shape and pose. In contrast, some datasets, like MHHI [133] and ExPI [70], adopt a different approach by constructing custom 3D human meshes from captured motion actors, achieving more realistic motion representation and better alignment between 3D meshes and visual data.

Text-Conditioned Human-human Datasets. Recent advances in multi-human interaction datasets have incorporated textual descriptions. Pioneering datasets like InterX [244] and InterHuman [124] feature human-generated natural language annotations that provide detailed descriptions of both actor and reactor movements at the body part level for specific interaction sequences. In contrast, LAION-Pose [185] and WebVid-Motion [185] take an automated approach, utilizing Visual Question Answering (VQA) through the Instruct-BLIP [42] model to generate captions. These automated annotations are obtained by prompting the model to "describe the person or group of people’s action and body poses in the image."

Audio-Conditioned Human-human Datasets. Several datasets extend beyond visual and textual modalities by integrating audio signals to enrich multimodal analysis. CMU-Panoptic [97] and Haggling [96] employ the same multi-camera system to capture synchronized audiovisual data. Haggling is specifically designed to record three-person conversations, enabling the study of social dynamics in negotiation scenarios, whereas CMU-

Panoptic expands its scope to include instrumentally performed music, background music, and noise generated by human motion. Talking With Hands 16.2M [114] emphasizes non-verbal communication by synchronizing conversational audio with detailed annotations of hand and body movements, supporting research on gesture and interaction analysis. Furthermore, DD100 [191] includes approximately two hours of professional dance performances, which capture various dance movements in different genres of background music, such as Samba and Tango.

5.2 Human-Object Interaction Datasets

Recent years have witnessed the emergence of diverse datasets specifically designed for 3D human-object interaction modeling, each addressing distinct aspects of interaction complexity. Table 6 presents comprehensive statistics of these human-object interaction datasets.

Grasping Hand Datasets. Hand-grasp datasets capture isolated instances of hand-object interaction, providing detailed annotations of grasp poses and contact points. These datasets are foundational for training and evaluating models on grasp synthesis and pose estimation. DexYCB [26] offers a comprehensive dataset with RGB-D images and 3D annotations of hand poses and object poses for 3D-printed objects from the YCB benchmark [20], facilitating studies on accurate grasp detection and pose estimation. ObMan [81] leverages synthetic data to simulate diverse hand-object interactions with MANO [179] hand models and object meshes,

Table 7: Human-scene interaction datasets. This table summarizes key statistics and features of various human-scene interaction datasets. Subjects: The number of individuals involved in the dataset; Sequences: The number of motion clips available; Frames: The total number of frames capturing 3D human motions; Length: The cumulative duration of the dataset’s motion data (in hours); Motion Acquisition: The method used to obtain motion data; Scene Acquisition: The method used to obtain scene data; Modality: The representation format of motion data; Dynamic: Indicates whether the dataset includes dynamic or static scene.

Dataset	Year	Venue	Subjects	Scenes	Sequences	Frames	Length	Motion Acquisition	Scene Acquisition	Modality	Condition	Video	Dynamic
LINGO [93]	2024	TOG	-	120	-	-	16h	MoCap	VR Environment	SMPL-X	Text	✓	✓
TRUMANS [95]	2024	CVPR	5	100	-	1.6M	15h	MoCap	VR Environment	SMPL-X	Action Label	✓	✓
LaserHuman [36]	2024	-	-	11	3374	-	3h	RGB + IMU	LiDAR	SMPL	Text	✓	✓
iReplica [74]	2024	3DV	8	7	-	680K	0.8h	IMU	-	SMPL	-	✓	✓
ParaHome [101]	2024	-	30	1	101	56M	7.3h	mRGB + IMU	Structured Light	SMPL-X	Text	✗	✓
CIRCLE [8]	2023	CVPR	5	9	7K	4.3M	10h	MoCap	VR Environment	SMPL-X	-	✗	✗
HUMANISE [234]	2022	NeurIPS	-	643	19.6K	1.2M	-	Alignment	mRGB-D	SMPL-X	Text	✗	✗
GIMO [280]	2022	ECCV	11	19	217	129K	-	IMU	Phone Scanned	SMPL-X	Gaze	✓	✗
EgoBody [266]	2022	ECCV	36	15	125	220K	-	mRGB-D	Phone Scanned	SMPL-X	Gaze	✓	✗
RICH [85]	2022	CVPR	22	5	142	577K	-	mRGB	Laser Scanned	SMPL-X	-	✓	✗
SAMP [78]	2021	ICCV	1	7	-	185K	1.6h	MoCap	CAD Model	SMPL-X	-	✗	✗
HPS [75]	2021	CVPR	7	8	-	300K	3h	IMU	-	SMPL	-	✗	✗
GTA-IM [21]	2020	ECCV	50	49	119	1.0M	-	GameEngine	Game Environment	3D skeleton	-	✓	✗
PROX [79]	2019	ICCV	20	12	60	100K	-	RGB	Structured Light	SMPL-X	-	✓	✗
i3DB [152]	2019	TOG	1	15	-	-	-	RGB	Optimization	3D skeleton	-	✓	✗
PiGraphs [182]	2016	TOG	5	30	63	100K	2h	RGB-D	mRGB-D	3D skeleton	Text	✗	✗

emphasizing the generation of realistic static grasps in controlled environments. ContactDB [14] provides high-resolution annotations of contact areas on hand and object surfaces, offering a tactile perspective to grasp modeling and enabling research on contact dynamics. These datasets focus on precise hand-object alignment, capturing essential spatial relationships that are critical for static grasp analysis and synthesis. Additionally, HO-3D [76] is the first markerless dataset of color images with 3D annotations of the hand and object, designed for benchmarking 3D hand-object pose estimation.

Whole Body HOI Datasets. Whole-body interaction datasets extend beyond hand-object interactions to capture the interplay between the entire human body and objects. GRAB [201] provides detailed 3D motion data of whole-body grasps, including articulated hands, body poses, and even facial expressions, while interacting with 51 everyday objects. It captures both static grasps and dynamic interactions, such as object handovers and usage, offering a comprehensive resource for modeling full-body grasping actions and contact dynamics. COUCH [269] and CHAIRS [94] target whole-body seated interactions, such as sitting, leaning, and adjusting posture while interacting with different types of furniture. They focus on contact points and posture dynamics, and provide fine-grained annotations for realistic full-body interactions in indoor settings. BEHAVE [13], HODome [260], InterCap [89], IMHD2 [274] capture full-body human-object interactions in natural environments using multi-view RGB-D recordings. They provide annotations for 3D human and object tracking, offering rich datasets for understanding naturalistic whole-body motion during interactions, such as carrying, pushing, and holding.

Articulated Object Interaction Datasets. ARCTIC [53] dataset is designed to study dexterous bimanual manipulation with articulated objects, addressing the complexities of handling objects with moving parts, such as laptops or scissors. It includes over 2.1 million RGB frames from multiple synchronized views, with paired 3D hand and object meshes for high-fidelity capture of hand-object interactions.

Text-Conditioned HOI Datasets. Text-conditioned HOI datasets provide multimodal data linking natural language descriptions to human-object interactions. HIMO [137] offers richly annotated sequences of full-body interactions with objects, paired with textual descriptions that capture detailed semantics and temporal progression, supporting tasks like text-to-motion synthesis and contextual interaction modeling. OMOMO [118] also aligns textual instructions with object-specific full-body interactions, focusing on generating diverse and realistic motions conditioned on language input and object properties. Semantic-HOI [250] is built by prompting GPT-4V [2] using hand-object images for annotations and includes fine-grained decoupled human pose descriptions.

5.3 Human-Scene Interaction Datasets

Technological advances in motion capture, virtual reality, and multi-modal data acquisition have enabled the development of diverse HSI datasets. These datasets can be classified into two main categories: interactions with *static scene* and interactions with *dynamic-involved scenes*. Table 7 provides detailed statistics of current HSI datasets in these two categories.

Table 8: **Human-mix interaction datasets.** This table summarizes key statistics and features of various human-mix interaction datasets. Tasks: Types of human interaction tasks—HHI: Human-Human Interaction, HOI: Human-Object Interaction; Subjects: The number of entities involved in the dataset; Sequences: The number of motion clips available; Frames: The total number of frames capturing 3D human motions; Length: The cumulative duration of the dataset’s motion data (in hours); Acquisition: The method used to obtain motion data; Modality: The representation format of motion data; Video, Text, Audio: Indicates whether the dataset includes corresponding modalities.

Dataset	Year	Venue	Tasks	Subjects	Sequences	Frames	Length	Acquisition	Modality	Video	Text	Audio
HOI-M ³ [261]	2024	CVPR	HHI, HOI	46 Human, 90 Objects	-	181M	20h	MoCap	SMPL	✓	✗	✗
HHOI [189]	2016	IJCAI	HHI, HOI	8 Human, 2 Objects	118	7.5K	0.2h	RGB-D	3D Skeleton	✓	✗	✗

Interaction with Static Scene. Static scene interaction datasets capture human behavior within fixed environments, focusing on interactions with stationary objects and unchanging scenes. These datasets vary in their capture methodologies and included modalities. Early datasets, like PiGraphs [182], establish foundations by capturing temporal interactions between humans and local object configurations. PROX [79] and i3DB [152] advance the field by providing RGB video-optimized human motion data, while GTA-IM [21] introduces synthetic data collection through game engine interfaces, incorporating RGB images, pose visualizations, and depth maps. SAMP [78] utilizes a pre-obtained CAD model and a motion capture device to obtain a diverse sitting scenario in the scene. Recent datasets have expanded to include multiple sensory modalities. HPS [75] employs head-mounted cameras for subject self-localization in large 3D scenes, while RICH [85] provides vertex-level contact labels and multi-view videos for detailed human-scene contact analysis. EgoBody [266] and GIMO [280] incorporate eye gaze data alongside third-person and egocentric views, with GIMO specifically focusing on leveraging gaze information to predict future body movements. HUMANISE [234] takes a novel approach by aligning pre-captured human motion sequences with scanned indoor scenes, additionally providing text descriptions of actions and interaction targets for multi-modal analysis. CIRCLE [8] focuses specifically on reaching motions in cluttered environments, utilizing virtual reality (VR) to present scenes to motion capture subjects.

Interaction with Dynamic Scene. Human interactions inherently modify their surrounding environments, creating dynamic and evolving scenes. To capture these complex interactions, several datasets have been introduced that document scenarios involving moving objects, scene modifications, and interactions with articulated entities. iReplica [74] provides comprehensive motion capture data while tracking environmental changes induced by human actions, such as table displacement and door manipulation. Complementing this, ParaHome [101] specializes in fine-grained interactions with small objects, documenting both body and finger motions alongside

dynamic changes in articulated objects—from laptop operations to stove control manipulation. LaserHuman [36] offers a unique perspective by combining human motion capture with free-form language descriptions of movements and environmental interactions. This dataset encompasses both indoor and expansive outdoor environments, representing dynamic scenes through LiDAR point cloud technology. TRUMANS [95] enhances the field by capturing diverse indoor activities with dynamic objects in a VR-assisted environment, providing frame-wise action labels for multi-modal analysis of activities such as bottle handling and refrigerator operation. Building upon these foundations, LINGO [93] stands as the most extensive human-scene interaction motion dataset to date. Utilizing VR-assisted capture techniques, it offers fully text-annotated documentation of diverse and extended human motions coupled with dynamic object interactions.

5.4 Human-Mix Interaction Datasets

Compared to datasets focusing on primary interactive tasks, datasets capturing multi-entity interactions remain limited in scope. Currently, only two datasets—HOI-M³ [261] and HHOI [189]—provide resources for studying human-human-object interactions. While HHOI is restricted to object root translation data, HOI-M³ offers comprehensive object mesh and motion information, enabling more sophisticated modeling of human-human-object interaction dynamics.

This scarcity presents significant opportunities for dataset development across various multi-entity scenarios, including human-human-object interactions, human-human-scene interactions, and complex human-human-object-scene combinations. A detailed comparison of existing human-mix interaction datasets is presented in Table 8.

6 Evaluation Metrics

Human interaction motion generation requires comprehensive evaluation across multiple dimensions. Current metrics assess three key aspects: *Fidelity*—the quality

Table 9: Overview of evaluation metrics for human interaction motion generation.

Category	Sub-category	Metrics
Fidelity	Comparison with Ground-Truth	MPJPE [90], MPJVE [60], Trajectory Error [99], Location Error [99], Average Error [99], Root Error [184], Pose Error [226], AFD [61], AME [70], VIM [4], VAM [4], VSM [4], NDMS [205], SSCP [206], SJP [12], PCK [5]
	Naturalness	FID (FVD) [82], Recognition Accuracy [69], MMD [138], Critic Accuracy [109], Critic Score [224]
	Physical Plausibility	Foot Skating Ratio [99]
Diversity	Inter-Motion	Diversity [69], Multimodality [69]
Condition Coherence	Partners' Motion-Conditioned	Mutual Consistency [203], BED [191], Contact Frequency [191]
	Object-Conditioned	CD [237], Contact Ratio [287], Penetration Depth/Volume/Percentage [287], Grasp Success Rate [17]
	Scene-Conditioned	Collision Ratio [8], Penetration Distance [277], Semantic Contact Score [276]
	Text-Conditioned	R-Precision [68], MultiModal Distance [68], EID [169]
	Audio-Conditioned	BAS [192], SSCA [96]
User Study	User Study	Preference [235], Rating (Motion Quality [60], Reaction Plausibility [60], Realness [226])

and naturalness of generated motions; *Diversity*—the variety of generated outputs; and *Condition Coherence*—the adherence to interaction constraints and task objectives. A comprehensive examination of evaluation metrics is presented in Table 9.

6.1 Interaction Motion Fidelity

Evaluating the fidelity of generated human interaction motions is crucial to ensuring their accuracy, realism, and physical plausibility. This section summarizes evaluation metrics for fidelity in three key aspects: *Comparison with ground-truth motions*, assessing generated motion using distance-based metrics; *Naturalness*, evaluating perceptual and statistical similarities between generated and real motions; and *Physical plausibility*, measuring adherence to real-world physical constraints and interaction dynamics.

6.1.1 Comparison with Ground-Truth

Fidelity in interactive human motion generation is predominantly evaluated by comparing generated motions with ground-truth motions using distance-based metrics, with Mean Per-Joint Positional Error (MPJPE) [90] serving as the primary measure. MPJPE quantifies the average spatial discrepancy between each corresponding joint in the predicted and actual poses, with lower values indicating higher fidelity. For a skeleton S and a frame f , MPJPE is calculated as

$$MPJPE(f, S) = \frac{1}{N_S} \sum_{i=1}^{N_S} \|m_{f,S}^{(f)}(i) - m_{gt,S}^{(f)}(i)\|_2, \quad (7)$$

where N_S represents the number of joints in skeleton S . When considering multiple frames, the overall error is obtained by averaging the MPJPE values across all frames.

In addition to MPJPE, other related metrics, such as Mean Per-Frame Per-Joint Velocity Error (MPJVE) [60], Aligned Mean Error (AME) [70], Trajectory Error [99],

Location Error [99], Average (Root) Error [99], Pose Error [226], Average Frame Distance (AFD) [61], Visibility-Ignored Metric (VIM) [4], and Visibility-Aware Metric (VAM) [4] are purposed as complementary metrics. These metrics similarly assess various aspects of distance, orientation, and trajectory between the generated and ground-truth motions, providing a comprehensive evaluation of location, pose, and movement accuracy under different conditions.

Beyond direct L2 distance computations, some evaluation metrics leverage more information to provide deeper insights. Visibility Score Metric (VSM) [4] assesses the precision of predicted visibility scores for all joints by measuring the average Intersection over Union (IoU) and F1 Scores of the joints, ensuring reliable visibility predictions in future frames. Normalized Directional Motion Similarity (NDMS) [205] evaluates the alignment of motion directions and the ratio of movement magnitudes between predicted and real motions. Symbolic Social Cues Protocol (SSCP) [206] examines the accuracy of social interactions within the generated motions, such as appropriate gestures for activities like talking or listening, aligning them with symbolic interaction states observed in the ground-truth. Salient Joints Precision (SJP) [12], measures the precision of predicted salient joints by comparing the generated sequence of important movement joints against the true sequence. Probability of Correct Keypoints (PCK) [5] determines the accuracy of location keypoint predictions by verifying if they fall within a defined radius around ground-truth positions, providing a probabilistic measure of keypoint localization accuracy.

6.1.2 Naturalness

Naturalness in human interaction motion generation assesses how lifelike and plausible the generated motions appear, often by comparing the statistical and perceptual properties of the generated motions to ground-truth motions.

Fréchet Inception Distance (FID) [82] and its video-adapted version, Fréchet Video Distance (FVD), have

been widely used in many works [60, 61, 72, 124, 169, 184, 191, 203, 235, 245, 246] to measure the divergence between the feature distributions of ground truth and generated motions. These metrics leverage deep features extracted from classification models to quantify the similarity between distributions. FID is calculated as:

$$\text{FID} = \|\mu_{gt} - \mu_{gen}\|_2^2 + \text{tr} \left(\mathbf{C}_{gt} + \mathbf{C}_{gen} - 2(\mathbf{C}_{gt} * \mathbf{C}_{gen})^{\frac{1}{2}} \right), \quad (8)$$

where μ_{gt} , μ_{gen} and \mathbf{C}_{gt} and \mathbf{C}_{gen} are the means and covariance matrices of the deep features extracted from ground truth and the generated motions respectively. The operator $\text{tr}(\cdot)$ denotes the trace of the matrix.

Additionally, Maximum Mean Discrepancy (MMD) [138] further assesses naturalness by evaluating the similarity between generated and real motion distributions either on a per-timestep basis (MMD-A) or across entire motion sequences (MMD-S) by flattening motion sequences into vector representations. Action Recognition Accuracy [69] uses classification models to determine whether the generated motions can be accurately identified as specific actions, thereby measuring their realism and semantic correctness. Critic Accuracy [109] employs an adversarial model to assess how easily a discriminator can distinguish between real and generated motions; lower critic accuracy indicates higher naturalness. Critic Score [224] is a data-driven metric that learns human perceptual preferences to evaluate the naturalness and quality of generated motions, demonstrating higher consistency with human preference evaluations than other metrics.

6.1.3 Physical Plausibility

Physical plausibility assesses how well the generated motions conform to realistic physical constraints and natural interaction dynamics. A common metric for this evaluation is the Foot Skating Ratio [99], which quantifies unintended foot sliding during motion, reflecting the stability and grounding of movements.

6.2 Diversity

In the evaluation of the diversity of generated motions, Diversity [69] and Multimodality [69] are critical metrics that assess different aspects of variation within the generated motions. Diversity refers to the variations among a set of generated motions, measuring the overall range and distinctness within the generated motion distribution. Diversity is calculated as:

$$\text{Diversity} = \frac{1}{S_d} \sum_{i=1}^{S_d} |v_i - v'_i|_2, \quad (9)$$

where S_d is the number of samples used in the experiments, v_i and v'_i are the deep feature vectors of the i -th samples from two randomly sampled subsets of generated motions, and $\|\cdot\|_2$ represents the L2 norm (Euclidean distance).

In contrast, Multimodality measures how much the generated motions diversify within each action type or text prompt, reflecting the model’s ability to produce multiple plausible variations for a single input. Given a set of motions with C action types, for the c -th action, two subsets with the same sample size S_l are randomly sampled. The multimodality is formalized as:

$$\text{Multimodality} = \frac{1}{C \times S_l} \sum_{c=1}^C \sum_{i=1}^{S_l} \|v_{c,i} - v'_{c,i}\|_2, \quad (10)$$

where $v_{c,i}$ and $v'_{c,i}$ are the deep feature vectors of the i -th samples from two randomly sampled subsets within the c -th action type.

In summary, Diversity ensures a wide range of motion variations, enriching the generated data, while Multimodality ensures the model can produce multiple plausible variations for a given input, enhancing its adaptability and usefulness in dynamic interactive scenarios.

6.3 Condition Coherence

Ensuring coherence in condition-driven human interaction motion generation is essential for producing coherent and contextually accurate interactions. This section evaluates condition coherence across multiple domains, including partners’ motion, object, scene, text, and audio.

6.3.1 Partners’ Motion-Conditioned

Partners’ motion-conditioned coherence focuses on ensuring that the generated motions adhere closely to the partner’s motions in terms of interaction coherence or rhythmic synchronization. One metric is Mutual Consistency [203], which assesses the coherence of interactions between actor and reactor motions by examining factors such as relative positions, action-reaction timings, and directional alignment. This metric employs a trained classification model to distinguish between consistent (correct and unmodified interactions) and inconsistent (randomly paired) motion pairs. Another metric is Beat Echo Degree (BED) [191], which quantifies the consistency of dynamic rhythms between two dancers. BED is calculated by first identifying the timing of beats in both the leader and follower movements through the detection of local minima in motion velocity. Mathematically,

BED is expressed as:

$$\text{BED} = \frac{1}{|B_l|} \sum_{t' \in B_l} \exp \left\{ -\frac{\min_{t_f \in B_f} \|t_l - t_f\|^2}{2\sigma^2} \right\}, \quad (11)$$

where B_l and B_f represent the sets of beat times for the leader and follower, respectively. σ , the parameter used for normalization, is set to 3 in Duolando [191].

In terms of measuring physical plausibility in HHI, Contact Frequency [191] can be used as a key metric that measures the frequency of physical interactions between individuals. Higher contact frequencies suggest more believable human-human interactions, as they align with the natural tendency for frequent contact in close interactions, such as dance or combat engagements.

6.3.2 Object-Conditioned

Evaluating human-object interaction requires metrics that rigorously assess both physical plausibility and the contact accuracy between humans and objects, particularly focusing on hand-object interactions where precise alignment is critical. Chamfer Distance [237] is widely used to measure the geometric consistency between predicted and ground-truth point clouds, making it effective in evaluating the accuracy of contact regions and the spatial alignment of hand poses with objects. Contact ratio [111, 287] directly measures the correctness of predicted contact points relative to ground-truth regions, reflecting how well the interaction captures realistic touch dynamics. To ensure physical plausibility, several penetration-related metrics are employed. Penetration Percentage [162] evaluates whether the signed distance between hand and object meshes exceeds a specified threshold (e.g. 1 mm), identifying the proportion of mesh points involved in penetrative errors. Penetration Volume [128, 287] quantifies the extent of penetration by voxelizing both hand and object meshes with 0.5 cm^3 patches, counting the intersecting voxels. Penetration Depth [131, 162, 287] computes the maximum distance from the intersected voxels to another mesh surface.

Additionally, Grasp Success Rate [17] serves as a dynamic evaluation metric, where a grasp is considered successful if the object remains stable—without falling to the ground or table—within a 0.5 second time window after the interaction. Another crucial metric is Simulation Displacement [287], which evaluates the stability of generated interactions by placing them in a physics simulation. By fixing the hand poses, this metric measures the displacement of the object’s center of mass under the influence of gravity over a fixed period.

6.3.3 Scene-Conditioned

Scene-conditioned coherence mainly focuses on evaluating the physical plausibility of human motion within a

given scene. The Collision Ratio [8] measures the frequency of body vertices or frames that penetrate the scene, highlighting the occurrence of physical rule violations. Penetration Distance [277] quantifies the extent of penetration, either as an average across all frames or as the maximum distance observed in a single frame. Together, these metrics provide insights into adherence to physical constraints in HSI scenarios.

Beyond physical rules, the Semantic Contact Score [276] evaluates how well-generated interactions align with action-specific body-scene contact semantics. It is computed as a weighted sum of binary contact features, with weights derived from action-specific body vertex contact probabilities.

6.3.4 Text-Conditioned

Text-conditioned coherence metrics measure the alignment between generated motions and provided textual descriptions. R-Precision [68] measures retrieval accuracy by ranking Euclidean distances between motion and text features within a dataset containing the ground truth and mismatched descriptions. It assesses precision at the top-1, top-2, and top-3 positions separately, determining how often the correct description is among the closest matches. MultiModal Distance [68] calculates the average Euclidean distance between the motion features of the generated motions and the text features of their corresponding descriptions, providing a direct measure of the feature space alignment between modalities. Additionally, Extrinsic Individual Diversity (EID) [169] measures how distinct textual descriptions influence the diversity of individual motion dynamics by comparing distributions of generated motions generated with original and randomly replaced descriptions via Wasserstein distance. A higher EID indicates greater control over the diversity of motions driven by individual textual inputs. When analyzed alongside other metrics like R-Precision and FID, EID helps assess the balance between individual diversity and interaction quality, ensuring that the generated motions are both varied and accurately conditioned on the provided text descriptions.

6.3.5 Audio-Conditioned

Audio-conditioned coherence emphasizes the alignment of generated motions with corresponding audio inputs, such as music rhythms or speech patterns. A key metric used to evaluate this alignment is the Beat-Align Score (BAS) [192], which assesses how well the generated motions synchronize with the rhythmic beats of the music. When the reference base is replaced with the leader’s dynamic beats, BAS is adapted to Beat Echo Degree (BED), as described partner’s motion-condition

coherence. Additionally, Speaking Status Classification Accuracy (SSCA) [96] measures the model’s ability to generate contextually appropriate motions that reflect the speaking status of the audio input. This metric involves classifying whether the generated motion corresponds to speaking or non-speaking states, ensuring that the motions are contextually appropriate and effectively represent audio-driven activities such as gestures associated with speech. These metrics provide diverse perspectives for assessing the model’s ability to generate contextually accurate and interactive human motions driven by audio input.

6.4 User Study

User studies play a crucial role in evaluating interactive human motion generation, particularly for assessing objectives that are challenging to quantify through automated metrics alone. These studies provide valuable insight into the subjective quality and perceptual aspects of generated motions. User studies can be broadly categorized into two major types. The first type involves eliciting user preferences [235] by comparing generated motions against baseline methods or ground-truth motions, allowing researchers to determine which motions are favored in terms of overall appeal and effectiveness. The second type requires participants to rate the generated motions on various dimensions, such as motion quality [60], reaction plausibility [60], and realism [226]. These ratings help in evaluating specific attributes of the generated motions, providing a nuanced understanding of their strengths and areas for improvement.

7 Conclusion and Outlook

In conclusion, this survey provides a systematic review of recent advances in human interaction motion generation, organized around four interaction categories: human-human, human-object, human-scene, and human-mix interactions. For each category, we examine methodological breakthroughs and classify approaches based on their solutions to core technical challenges. We analyze the distinctive characteristics of relevant datasets and their contributions to the advancement of the field. In addition, we present a unified framework for evaluating different interaction tasks through standardized metrics. Given the rapid evolution of this field, we identify and discuss four promising research directions that warrant further investigation.

Data. Acquiring high-quality human interaction data presents significant challenges and costs. For instance,

capturing human-scene interactions requires either comprehensive scene scanning or the meticulous reconstruction of virtual 3D scene layouts in physical spaces, followed by motion capture and coordinate system calibration [93, 95]. While recent datasets have documented diverse human interactions in controlled environments, they struggle to encompass the full spectrum of real-world interaction scenarios. Several promising approaches could address these limitations. First, more efficient motion capture technologies, such as IMU sensors, could provide a trade-off between data quality and coverage. Second, leveraging heterogeneous data sources could enhance motion modeling; for example, generative motion priors could be learned from large-scale datasets of isolated motions. These motion priors can be further applied to interacting with other entities. Additionally, LLMs and VLMs, which encode rich knowledge of human interactions, could help overcome the data scarcity challenge while improving flexibility and generalizability.

Physical Plausibility. Current approaches for generating interactive motions face challenges in achieving physical plausibility, such as accurately representing gravity, force interactions, and texture responses. Physics simulator-based methods [240] offer a partial solution to these challenges; they typically rely on reinforcement learning frameworks that use physical feedback as rewards for motion correction. However, these approaches have limitations: they are often constrained to specific actions and struggle to generalize to novel motions. Furthermore, they exhibit limited compatibility with expressive generative models such as diffusion models. Future research directions may investigate hybrid approaches that combine the physical accuracy of simulator-based methods with the flexibility and generative capabilities of modern deep learning architectures.

Representation. Efficient data representation of motions, 3D objects, and scenes plays a crucial role in interaction motion generation. An effective representation framework for interaction scenarios must capture both intrinsic properties (e.g. motion joint positions, object geometry) and relational information between interacting entities. In human-human interactions, Sebastian et al. [197, 198] demonstrate this by extracting extensive motion features of characters relative to their opponents to characterize interaction dependencies. Similarly, for human-object interactions, InterDiff [247] reveals that object motions relative to contact points, rather than world origins, exhibit more learnable patterns. The representation of 3D objects and scenes presents additional challenges due to their inherent complexity: they comprise thousands of unordered points and faces that lack

well-defined structural representation. This challenge is particularly pronounced in human-scene interactions, where the scale of 3D geometric elements becomes intractable, compounded by the need to represent spatial layouts and regional semantic information. Given the limited availability of high-quality human interaction data, developing efficient, interaction-aware feature representations becomes paramount.

Editing and Controllability. The ability to edit interactions and precisely control their generation is crucial for practical applications. While several techniques have been developed for single-person motion generation—including joint trajectory-based control [167, 241], stylized generation [281], and text-prompted editing [10]—these approaches have yet to be effectively adapted for human interaction scenarios. We believe these investigations could bring our interaction generation researches closer to real-world applications such as animations and robotics.

Data Availability Statement

This study is a survey and does not involve the generation or analysis of new datasets. All referenced datasets are available from their original sources. The details of all referred works are also provided in this public GitHub repository: <https://github.com/soraproducer/Awesome-Human-Interaction-Motion-Generation>.

References

- van der Aa, N., Luo, X., Giezeman, G., Tan, R., Veltkamp, R.: Umpm benchmark: A multi-person dataset with synchronized video and motion capture data for evaluation of articulated human motion and interaction. In: 2011 IEEE International Conference on Computer Vision Workshops (ICCV Workshops), pp. 1264–1269 (2011). DOI 10.1109/ICCVW.2011.6130396 **16**
- Achiam, J., Adler, S., Agarwal, S., Ahmad, L., Akkaya, I., Aleman, F.L., Almeida, D., Altenschmidt, J., Altman, S., Anadkat, S., et al.: Gpt-4 technical report. arXiv preprint arXiv:2303.08774 (2023) **6, 18**
- Adeli, V., Adeli, E., Reid, I., Niebles, J.C., Rezatofghi, H.: Socially and contextually aware human motion and pose forecasting. IEEE Robotics and Automation Letters **5**(4), 6033–6040 (2020) **5, 8**
- Adeli, V., Ehsanpour, M., Reid, I., Niebles, J.C., Savarese, S., Adeli, E., Rezatofghi, H.: Tripod: Human trajectory and pose dynamics forecasting in the wild. In: 2021 IEEE/CVF International Conference on Computer Vision (ICCV). IEEE (2021). DOI 10.1109/iccv48922.2021.01314. URL <http://dx.doi.org/10.1109/ICCV48922.2021.01314> **5, 8, 20**
- Ahuja, C., Ma, S., Morency, L.P., Sheikh, Y.: To react or not to react: End-to-end visual pose forecasting for personalized avatar during dyadic conversations (2019). URL <https://arxiv.org/abs/1910.02181> **4, 8, 9, 20**
- Akber, S.M.A., Kazmi, S.N., Mohsin, S.M., Szcześna, A.: Deep learning-based motion style transfer tools, techniques and future challenges. Sensors **23**(5) (2023). DOI 10.3390/s23052597. URL <https://www.mdpi.com/1424-8220/23/5/2597> **2**
- Alexanderson, S., Nagy, R., Beskow, J., Henter, G.E.: Listen, denoise, action! audio-driven motion synthesis with diffusion models. ACM Transactions on Graphics (TOG) **42**(4), 1–20 (2023) **2**
- Araujo, J.P., Li, J., Vetrivel, K., Agarwal, R., Gopinath, D., Wu, J., Clegg, A., Liu, C.K.: Circle: Capture in rich contextual environments (2023). URL <https://arxiv.org/abs/2303.17912> **4, 5, 11, 13, 14, 18, 19, 20, 22**
- Arikan, O., Forsyth, D.A., O’Brien, J.F.: Motion synthesis from annotations. In: ACM SIGGRAPH 2003 Papers, pp. 402–408 (2003) **1**
- Athanasidou, N., Cseke, A., Diomataris, M., Black, M.J., Varol, G.: Motionfix: Text-driven 3d human motion editing. In: SIGGRAPH Asia 2024 Conference Papers, pp. 1–11 (2024) **24**
- Badler, N.I., Palmer, M.S., Bindiganavale, R.: Animation control for real-time virtual humans. Communications of the ACM **42**(8), 64–73 (1999) **1**
- Baruah, M., Banerjee, B.: A multimodal predictive agent model for human interaction generation. In: Proceedings of the IEEE/CVF Conference on Computer Vision and Pattern Recognition (CVPR) Workshops (2020) **5, 7, 8, 20**
- Bhatnagar, B.L., Xie, X., Petrov, I.A., Sminchisescu, C., Theobalt, C., Pons-Moll, G.: Behave: Dataset and method for tracking human object interactions. In: Proceedings of the IEEE/CVF Conference on Computer Vision and Pattern Recognition, pp. 15935–15946 (2022) **11, 17, 18**
- Brahmbhatt, S., Ham, C., Kemp, C.C., Hays, J.: Contactdb: Analyzing and predicting grasp contact via thermal imaging. In: Proceedings of the IEEE/CVF Conference on Computer Vision and Pattern Recognition (CVPR) (2019) **17, 18**
- Brahmbhatt, S., Handa, A., Hays, J., Fox, D.: Contactgrasp: Functional multi-finger grasp synthesis from contact. In: 2019 IEEE/RSJ International Conference on Intelligent Robots and Systems (IROS), pp. 2386–2393. IEEE (2019) **11**
- Brahmbhatt, S., Tang, C., Twigg, C.D., Kemp, C.C., Hays, J.: Contactpose: A dataset of grasps with object contact and hand pose. In: Computer Vision—ECCV 2020: 16th European Conference, Glasgow, UK, August 23–28, 2020, Proceedings, Part XIII 16, pp. 361–378. Springer (2020) **11, 17**
- Braun, J., Christen, S., Kocabas, M., Aksan, E., Hilliges, O.: Physically plausible full-body hand-object interaction synthesis. In: International Conference on 3D Vision (3DV) (2024) **5, 11, 12, 20, 22**
- Brown, T., Mann, B., Ryder, N., Subbiah, M., Kaplan, J.D., Dhariwal, P., Neelakantan, A., Shyam, P., Sastry, G., Askell, A., et al.: Language models are few-shot learners. Advances in neural information processing systems **33**, 1877–1901 (2020) **1, 6**
- Calli, B., Singh, A., Walsman, A., Srinivasa, S., Abbeel, P., Dollar, A.M.: The ycb object and model set: Towards common benchmarks for manipulation research. In: 2015 international conference on advanced robotics (ICAR), pp. 510–517. IEEE (2015) **11**
- Calli, B., Walsman, A., Singh, A., Srinivasa, S., Abbeel, P., Dollar, A.M.: Benchmarking in manipulation research:

- The ycb object and model set and benchmarking protocols. arXiv preprint arXiv:1502.03143 (2015) **17**
21. Cao, Z., Gao, H., Mangalam, K., Cai, Q., Vo, M., Malik, J.: Long-term human motion prediction with scene context (2020) **4, 13, 15, 18, 19**
 22. Cen, Z., Pi, H., Peng, S., Shen, Z., Yang, M., Shuai, Z., Bao, H., Zhou, X.: Generating human motion in 3d scenes from text descriptions. In: CVPR (2024) **13, 15**
 23. Cha, J., Kim, J., Yoon, J.S., Baek, S.: Text2hoi: Text-guided 3d motion generation for hand-object interaction. In: Proceedings of the IEEE/CVF Conference on Computer Vision and Pattern Recognition, pp. 1577–1585 (2024) **6, 10, 11**
 24. Chang, H., Zhang, H., Jiang, L., Liu, C., Freeman, W.T.: Maskgit: Masked generative image transformer. In: Proceedings of the IEEE/CVF Conference on Computer Vision and Pattern Recognition, pp. 11315–11325 (2022) **6**
 25. Chao, Y.W., Liu, Y., Liu, X., Zeng, H., Deng, J.: Learning to detect human-object interactions. In: 2018 IEEE winter conference on applications of computer vision (wacv), pp. 381–389. IEEE (2018) **11**
 26. Chao, Y.W., Yang, W., Xiang, Y., Molchanov, P., Handa, A., Tremblay, J., Narang, Y.S., Van Wyk, K., Iqbal, U., Birchfield, S., et al.: Dexycb: A benchmark for capturing hand grasping of objects. In: Proceedings of the IEEE/CVF Conference on Computer Vision and Pattern Recognition, pp. 9044–9053 (2021) **11, 17**
 27. Chen, J., Hu, P., Chang, X., Shi, Z., Kampffmeyer, M., Liang, X.: Sitcom-crafter: A plot-driven human motion generation system in 3d scenes. arXiv preprint arXiv:2410.10790 (2024) **15**
 28. Chen, S., Wu, A., Liu, C.K.: Synthesizing dexterous nonprehensile pregrasp for ungraspable objects. In: ACM SIGGRAPH 2023 Conference Proceedings, pp. 1–10 (2023) **11, 12**
 29. Chen, X., Jiang, B., Liu, W., Huang, Z., Fu, B., Chen, T., Yu, G.: Executing your commands via motion diffusion in latent space. In: Proceedings of the IEEE/CVF Conference on Computer Vision and Pattern Recognition, pp. 18000–18010 (2023) **2**
 30. Chen, Y., Tian, Y., He, M.: Monocular human pose estimation: A survey of deep learning-based methods. *Computer Vision and Image Understanding* **192**, 102897 (2020). DOI [10.1016/j.cviu.2019.102897](https://doi.org/10.1016/j.cviu.2019.102897). URL <http://dx.doi.org/10.1016/j.cviu.2019.102897> **2**
 31. Cho, K., van Merriënboer, B., Gulcehre, C., Bahdanau, D., Bougares, F., Schwenk, H., Bengio, Y.: Learning phrase representations using rnn encoder-decoder for statistical machine translation (2014). URL <https://arxiv.org/abs/1406.1078> **5**
 32. Chopin, B., Tang, H., Othberdout, N., Daoudi, M., Sebe, N.: Interaction transformer for human reaction generation (2023). URL <https://arxiv.org/abs/2207.01685> **6, 8, 10**
 33. Christen, S., Hampali, S., Sener, F., Remelli, E., Hodan, T., Sauser, E., Ma, S., Tekin, B.: Diffh2o: Diffusion-based synthesis of hand-object interactions from textual descriptions. In: SIGGRAPH Asia 2024 Conference Papers (2024) **6, 10, 11**
 34. Christen, S., Kocabas, M., Aksan, E., Hwangbo, J., Song, J., Hilliges, O.: D-grasp: Physically plausible dynamic grasp synthesis for hand-object interactions. In: Proceedings of the IEEE/CVF Conference on Computer Vision and Pattern Recognition (CVPR) (2022) **5, 6, 11, 12**
 35. Clark, A.: Being there: Putting brain, body, and world together again. MIT press (1998) **1**
 36. Cong, P., Wang, Z., Dou, Z., Ren, Y., Yin, W., Cheng, K., Sun, Y., Long, X., Zhu, X., Ma, Y.: Laserhuman: Language-guided scene-aware human motion generation in free environment (2024) **4, 13, 18, 19**
 37. Corona, E., Pumarola, A., Alenya, G., Moreno-Noguer, F., Rogez, G.: Ganhand: Predicting human grasp affordances in multi-object scenes. In: Proceedings of the IEEE/CVF conference on computer vision and pattern recognition, pp. 5031–5041 (2020) **11**
 38. Croitoru, F.A., Hondru, V., Ionescu, R.T., Shah, M.: Diffusion models in vision: A survey. *IEEE Transactions on Pattern Analysis and Machine Intelligence* **45**(9), 10850–10869 (2023) **1**
 39. Dabral, R., Shimada, S., Jain, A., Theobalt, C., Golyanik, V.: Gravity-aware monocular 3d human-object reconstruction. In: International Conference on Computer Vision (ICCV) (2021) **11, 17**
 40. Dai, A., Chang, A.X., Savva, M., Halber, M., Funkhouser, T., Nießner, M.: Scannet: Richly-annotated 3d reconstructions of indoor scenes. In: Proc. Computer Vision and Pattern Recognition (CVPR), IEEE (2017) **4**
 41. Dai, S., Li, W., Sun, H., Huang, H., Ma, C., Huang, H., Xu, K., Hu, R.: Interfusion: Text-driven generation of 3d human-object interaction. In: ECCV (2024) **10, 11**
 42. Dai, W., Li, J., Li, D., Tiong, A., Zhao, J., Wang, W., Li, B., Fung, P., Hoi, S.: Instructblip: Towards general-purpose vision-language models with instruction tuning. arXiv preprint arXiv:2305.06500 **2** (2023) **17**
 43. Denninger, M., Sundermeyer, M., Winkelbauer, D., Olefir, D., Hodan, T., Zidan, Y., Elbadrawy, M., Knauer, M., Katam, H., Lodhi, A.: Blenderproc: Reducing the reality gap with photorealistic rendering. In: 16th Robotics: Science and Systems, RSS 2020, Workshops (2020) **4**
 44. Dhariwal, P., Jun, H., Payne, C., Kim, J.W., Radford, A., Sutskever, I.: Jukebox: A generative model for music. arXiv preprint arXiv:2005.00341 (2020) **1**
 45. Diller, C., Dai, A.: Cg-hoi: Contact-guided 3d human-object interaction generation. In: Proc. Computer Vision and Pattern Recognition (CVPR), IEEE (2024) **11**
 46. Dilokthanakul, N., Mediano, P.A., Garnelo, M., Lee, M.C., Salimbeni, H., Arulkumaran, K., Shanahan, M.: Deep unsupervised clustering with gaussian mixture variational autoencoders. arXiv preprint arXiv:1611.02648 (2016) **8**
 47. Dosovitskiy, A., Beyer, L., Kolesnikov, A., Weissenborn, D., Zhai, X., Unterthiner, T., Dehghani, M., Minderer, M., Heigold, G., Gelly, S., Uszkoreit, J., Houlsby, N.: An image is worth 16x16 words: Transformers for image recognition at scale (2021). URL <https://arxiv.org/abs/2010.11929> **4, 14**
 48. Ebrahim, M.A.B.: 3d laser scanners’ techniques overview. *Int J Sci Res* **4**(10), 323–331 (2015) **3**
 49. Elhayek, A., de Aguiar, E., Jain, A., Tompson, J., Pishchulin, L., Andriluka, M., Bregler, C., Schiele, B., Theobalt, C.: Efficient convnet-based marker-less motion capture in general scenes with a low number of cameras. In: Proceedings of the IEEE Conference on Computer Vision and Pattern Recognition (CVPR) (2015) **16**
 50. Eyben, F., Wenginger, F., Gross, F., Schuller, B.: Recent developments in opensmile, the munich open-source multimedia feature extractor. In: Proceedings of the 21st ACM international conference on Multimedia, pp. 835–838 (2013) **4**
 51. Fabbri, M., Lanzi, F., Calderara, S., Palazzi, A., Vezzani, R., Cucchiara, R.: Learning to detect and track visible and occluded body joints in a virtual world (2018). URL <https://arxiv.org/abs/1803.08319> **16**

52. Fan, K., Tang, J., Cao, W., Yi, R., Li, M., Gong, J., Zhang, J., Wang, Y., Wang, C., Ma, L.: Freemotion: A unified framework for number-free text-to-motion synthesis (2024). URL <https://arxiv.org/abs/2405.15763> **4**, **6**, **7**, **8**, **9**
53. Fan, Z., Taheri, O., Tzionas, D., Kocabas, M., Kaufmann, M., Black, M.J., Hilliges, O.: Arctic: A dataset for dexterous bimanual hand-object manipulation. In: Proceedings of the IEEE/CVF Conference on Computer Vision and Pattern Recognition, pp. 12943–12954 (2023) **4**, **11**, **17**, **18**
54. Fieraru, M., Zanfir, M., Oneata, E., Popa, A.I., Olaru, V., Sminchisescu, C.: Three-dimensional reconstruction of human interactions. In: Proceedings of the IEEE/CVF Conference on Computer Vision and Pattern Recognition (CVPR) (2020) **8**, **16**
55. Furtado, J.S., Liu, H.H., Lai, G., Lacheray, H., Desouza-Coelho, J.: Comparative analysis of optitrack motion capture systems. In: Advances in Motion Sensing and Control for Robotic Applications: Selected Papers from the Symposium on Mechatronics, Robotics, and Control (SMRC'18)-CSME International Congress 2018, May 27-30, 2018 Toronto, Canada, pp. 15–31. Springer (2019) **3**
56. Gao, X., Yang, Y., Wu, Y., Du, S., Qi, G.J.: Multi-condition latent diffusion network for scene-aware neural human motion prediction (2024). URL <https://arxiv.org/abs/2405.18700> **13**, **14**
57. Garcia-Hernando, G., Yuan, S., Baek, S., Kim, T.K.: First-person hand action benchmark with rgb-d videos and 3d hand pose annotations. In: Proceedings of the IEEE conference on computer vision and pattern recognition, pp. 409–419 (2018) **11**
58. van Gemeren, C., Poppe, R., Veltkamp, R.C.: Spatio-temporal detection of fine-grained dyadic human interactions. In: M. Chetouani, J. Cohn, A.A. Salah (eds.) Human Behavior Understanding, pp. 116–133. Springer International Publishing, Cham (2016) **16**
59. Ghosh, A., Dabral, R., Golyanik, V., Theobalt, C., Slusallek, P.: Imos: Intent-driven full-body motion synthesis for human-object interactions. In: Eurographics (2023) **5**, **6**, **10**, **11**
60. Ghosh, A., Dabral, R., Golyanik, V., Theobalt, C., Slusallek, P.: Remos: 3d motion-conditioned reaction synthesis for two-person interactions (2024). URL <https://arxiv.org/abs/2311.17057> **6**, **7**, **8**, **9**, **10**, **16**, **20**, **21**, **23**
61. Goel, A., Men, Q., Ho, E.S.L.: Interaction mix and match: Synthesizing close interaction using conditional hierarchical gan with multi-hot class embedding (2022). URL <https://arxiv.org/abs/2208.00774> **5**, **8**, **20**, **21**
62. Gong, J., Zhang, C., Liu, F., Fan, K., Zhou, Q., Tan, X., Zhang, Z., Xie, Y., Ma, L.: Diffusion implicit policy for unpaired scene-aware motion synthesis. arXiv e-prints (2024) **13**, **15**
63. Gong, K., Lian, D., Chang, H., Guo, C., Jiang, Z., Zuo, X., Mi, M.B., Wang, X.: Tm2d: Bimodality driven 3d dance generation via music-text integration. In: Proceedings of the IEEE/CVF International Conference on Computer Vision, pp. 9942–9952 (2023) **2**
64. Goodfellow, I., Pouget-Abadie, J., Mirza, M., Xu, B., Warde-Farley, D., Ozair, S., Courville, A., Bengio, Y.: Generative adversarial networks. Communications of the ACM **63**(11), 139–144 (2020) **5**
65. Grady, P., Tang, C., Twigg, C.D., Vo, M., Brahmabhatt, S., Kemp, C.C.: Contactopt: Optimizing contact to improve grasps. In: Proceedings of the IEEE/CVF Conference on Computer Vision and Pattern Recognition (CVPR), pp. 1471–1481 (2021) **11**
66. Gui, J., Sun, Z., Wen, Y., Tao, D., Ye, J.: A review on generative adversarial networks: Algorithms, theory, and applications. IEEE transactions on knowledge and data engineering **35**(4), 3313–3332 (2021) **1**, **5**
67. Guo, C., Zou, S., Zuo, X., Wang, S., Ji, W., Li, X., Cheng, L.: Generating diverse and natural 3d human motions from text. In: Proceedings of the IEEE/CVF Conference on Computer Vision and Pattern Recognition, pp. 5152–5161 (2022) **2**
68. Guo, C., Zou, S., Zuo, X., Wang, S., Ji, W., Li, X., Cheng, L.: Generating diverse and natural 3d human motions from text. In: Proceedings of the IEEE/CVF Conference on Computer Vision and Pattern Recognition (CVPR), pp. 5152–5161 (2022) **8**, **13**, **20**, **22**
69. Guo, C., Zuo, X., Wang, S., Zou, S., Sun, Q., Deng, A., Gong, M., Cheng, L.: Action2motion: Conditioned generation of 3d human motions. In: Proceedings of the 28th ACM International Conference on Multimedia, pp. 2021–2029 (2020) **2**, **8**, **20**, **21**
70. Guo, W., Bie, X., Alameda-Pineda, X., Moreno-Noguer, F.: Multi-person extreme motion prediction. In: Proceedings of the IEEE/CVF conference on computer vision and pattern recognition, pp. 13053–13064 (2022) **8**, **16**, **17**, **20**
71. Guo, Y., Wang, H., Hu, Q., Liu, H., Liu, L., Bennamoun, M.: Deep learning for 3d point clouds: A survey. IEEE transactions on pattern analysis and machine intelligence **43**(12), 4338–4364 (2020) **4**
72. Gupta, D., Maheshwari, S., Kalakonda, S.S., Vaidyula, M., Sarvadevabhatla, R.K.: Dsag: A scalable deep framework for action-conditioned multi-actor full body motion synthesis. In: Proceedings of the IEEE/CVF Winter Conference on Applications of Computer Vision (WACV), pp. 4300–4308 (2023) **5**, **6**, **8**, **9**, **21**
73. Gupta, S., Malik, J.: Visual semantic role labeling. arXiv preprint arXiv:1505.04474 (2015) **11**
74. Guzov, V., Chibane, J., Marin, R., He, Y., Saracoglu, Y., Sattler, T., Pons-Moll, G.: Interaction replica: Tracking human-object interaction and scene changes from human motion. In: International Conference on 3D Vision (3DV) (2024) **18**, **19**
75. Guzov, V., Mir, A., Sattler, T., Pons-Moll, G.: Human positioning system (hps): 3d human pose estimation and self-localization in large scenes from body-mounted sensors. In: IEEE Conference on Computer Vision and Pattern Recognition (CVPR). IEEE (2021) **18**, **19**
76. Hampali, S., Rad, M., Oberweger, M., Lepetit, V.: Honnotate: A method for 3d annotation of hand and object poses. In: Proceedings of the IEEE/CVF conference on computer vision and pattern recognition, pp. 3196–3206 (2020) **11**, **17**, **18**
77. Hampali, S., Sarkar, S.D., Rad, M., Lepetit, V.: Keypoint transformer: Solving joint identification in challenging hands and object interactions for accurate 3d pose estimation. In: Proceedings of the IEEE/CVF Conference on Computer Vision and Pattern Recognition, pp. 11090–11100 (2022) **17**
78. Hassan, M., Ceylan, D., Villegas, R., Saito, J., Yang, J., Zhou, Y., Black, M.J.: Stochastic scene-aware motion prediction. In: Proceedings of the IEEE/CVF International Conference on Computer Vision, pp. 11374–11384 (2021) **13**, **18**, **19**
79. Hassan, M., Choutas, V., Tzionas, D., Black, M.J.: Resolving 3D human pose ambiguities with 3D scene constraints. In: International Conference on Computer Vi-

- sion (2019). URL <https://prox.is.tue.mpg.de> **4**, **13**, **18**, **19**
80. Hassan, M., Guo, Y., Wang, T., Black, M., Fidler, S., Peng, X.B.: Synthesizing physical character-scene interactions (2023). URL <https://arxiv.org/abs/2302.00883> **6**, **13**, **14**
 81. Hasson, Y., Varol, G., Tzionas, D., Kalevatykh, I., Black, M.J., Laptev, I., Schmid, C.: Learning joint reconstruction of hands and manipulated objects. In: CVPR (2019) **11**, **17**
 82. Heusel, M., Ramsauer, H., Unterthiner, T., Nessler, B., Hochreiter, S.: Gans trained by a two time-scale update rule converge to a local nash equilibrium. In: I. Guyon, U.V. Luxburg, S. Bengio, H. Wallach, R. Fergus, S. Vishwanathan, R. Garnett (eds.) *Advances in Neural Information Processing Systems*, vol. 30. Curran Associates, Inc. (2017). URL https://proceedings.neurips.cc/paper_files/paper/2017/file/8a1d694707eb0fefef65871369074926d-Paper.pdf **20**
 83. Ho, J., Jain, A., Abbeel, P.: Denoising diffusion probabilistic models. *Advances in neural information processing systems* **33**, 6840–6851 (2020) **6**
 84. Hu, T., Zhu, X., Su, K.: Efficient interaction recognition through positive action representation. *Mathematical Problems in Engineering* **2013**, 1–11 (2013). DOI 10.1155/2013/795360 **8**, **16**
 85. Huang, C.H.P., Yi, H., Höschle, M., Safroshkin, M., Alexiadis, T., Polikovskiy, S., Scharstein, D., Black, M.J.: Capturing and inferring dense full-body human-scene contact. In: *Proceedings IEEE/CVF Conf. on Computer Vision and Pattern Recognition (CVPR)*, pp. 13274–13285 (2022) **18**, **19**
 86. Huang, C.Z.A., Vaswani, A., Uszkoreit, J., Shazeer, N., Simon, I., Hawthorne, C., Dai, A.M., Hoffman, M.D., Dinculescu, M., Eck, D.: Music transformer. arXiv preprint arXiv:1809.04281 (2018) **1**
 87. Huang, D.A., Kitani, K.M.: Action-reaction: Forecasting the dynamics of human interaction. In: *European Conference on Computer Vision* (2014). URL <https://api.semanticscholar.org/CorpusID:518253> **5**, **8**
 88. Huang, S., Wang, Z., Li, P., Jia, B., Liu, T., Zhu, Y., Liang, W., Zhu, S.C.: Diffusion-based generation, optimization, and planning in 3d scenes. arXiv preprint arXiv:2301.06015 (2023) **13**, **14**
 89. Huang, Y., Taheri, O., Black, M.J., Tzionas, D.: Intercap: Joint markerless 3d tracking of humans and objects in interaction. In: DAGM German Conference on Pattern Recognition, pp. 281–299. Springer (2022) **11**, **17**, **18**
 90. Ionescu, C., Papava, D., Olaru, V., Sminchisescu, C.: Human3.6m: Large scale datasets and predictive methods for 3d human sensing in natural environments. *IEEE transactions on pattern analysis and machine intelligence* **36**(7), 1325–1339 (2013) **8**, **20**
 91. Javed, M.G., Guo, C., Cheng, L., Li, X.: Intermask: 3d human interaction generation via collaborative masked modelling. arXiv preprint arXiv:2410.10010 (2024) **6**, **7**, **9**
 92. Ji, Y., Xu, F., Yang, Y., Shen, F., Shen, H.T., Zheng, W.S.: A large-scale varying-view rgb-d action dataset for arbitrary-view human action recognition (2019). URL <https://arxiv.org/abs/1904.10681> **8**
 93. Jiang, N., He, Z., Wang, Z., Li, H., Chen, Y., Huang, S., Zhu, Y.: Autonomous character-scene interaction synthesis from text instruction (2024). URL <https://arxiv.org/abs/2410.03187> **4**, **6**, **12**, **13**, **14**, **15**, **18**, **19**, **23**
 94. Jiang, N., Liu, T., Cao, Z., Cui, J., Zhang, Z., Chen, Y., Wang, H., Zhu, Y., Huang, S.: Full-body articulated human-object interaction. In: *Proceedings of the IEEE/CVF International Conference on Computer Vision*, pp. 9365–9376 (2023) **4**, **11**, **17**, **18**
 95. Jiang, N., Zhang, Z., Li, H., Ma, X., Wang, Z., Chen, Y., Liu, T., Zhu, Y., Huang, S.: Scaling up dynamic human-scene interaction modeling. In: *Proceedings of the IEEE/CVF Conference on Computer Vision and Pattern Recognition*, pp. 1737–1747 (2024) **3**, **4**, **13**, **14**, **18**, **19**, **23**
 96. Joo, H., Simon, T., Cikara, M., Sheikh, Y.: Towards social artificial intelligence: Nonverbal social signal prediction in a triadic interaction (2019). URL <https://arxiv.org/abs/1906.04158> **8**, **9**, **16**, **17**, **20**, **23**
 97. Joo, H., Simon, T., Li, X., Liu, H., Tan, L., Gui, L., Banerjee, S., Godisart, T., Nabbe, B., Matthews, I., Kanade, T., Nobuhara, S., Sheikh, Y.: Panoptic studio: A massively multiview system for social interaction capture (2016). URL <https://arxiv.org/abs/1612.03153> **16**, **17**
 98. Karras, T.: A style-based generator architecture for generative adversarial networks. arXiv preprint arXiv:1812.04948 (2019) **1**
 99. Karunratanakul, K., Preechakul, K., Suwajanakorn, S., Tang, S.: Guided motion diffusion for controllable human motion synthesis (2023). URL <https://arxiv.org/abs/2305.12577> **2**, **20**, **21**
 100. Karunratanakul, K., Yang, J., Zhang, Y., Black, M., Muandet, K., Tang, S.: Grasping field: Learning implicit representations for human grasps. In: *2020 International Conference on 3D Vision (3DV 2020)*, pp. 333–344. IEEE, Piscataway, NJ (2020). DOI 10.1109/3DV50981.2020.00043 **12**
 101. Kim, J., Kim, J., Na, J., Joo, H.: Parahome: Parameterizing everyday home activities towards 3d generative modeling of human-object interactions (2024) **4**, **18**, **19**
 102. Kim, S., Kim, C., You, B., Oh, S.: Stable whole-body motion generation for humanoid robots to imitate human motions. In: *2009 IEEE/RSJ International Conference on Intelligent Robots and Systems*, pp. 2518–2524. IEEE (2009) **1**
 103. Kingma, D.P.: Auto-encoding variational bayes. arXiv preprint arXiv:1312.6114 (2013) **1**, **5**
 104. Kocabas, M., Athanasiou, N., Black, M.J.: Vibe: Video inference for human body pose and shape estimation. In: *Proceedings of the IEEE/CVF conference on computer vision and pattern recognition*, pp. 5253–5263 (2020) **3**
 105. Kong, Y., Fu, Y.: Human action recognition and prediction: A survey (2022). URL <https://arxiv.org/abs/1806.11230> **2**
 106. Kovar, L., Gleicher, M., Pighin, F.: Motion graphs. In: *Seminal Graphics Papers: Pushing the Boundaries, Volume 2*, pp. 723–732 (2023) **5**
 107. Kratzer, P., Bihlmaier, S., Midlagajni, N.B., Prakash, R., Toussaint, M., Mainprice, J.: Mogaze: A dataset of full-body motions that includes workspace geometry and eye-gaze. *IEEE Robotics and Automation Letters* **6**(2), 367–373 (2020) **11**
 108. Kulkarni, N., Rempe, D., Genova, K., Kundu, A., Johnson, J., Fouhey, D., Guibas, L.: Nifty: Neural object interaction fields for guided human motion synthesis. In: *Proceedings of the IEEE/CVF Conference on Computer Vision and Pattern Recognition*, pp. 947–957 (2024) **10**, **11**, **12**
 109. Kundu, J.N., Buckchash, H., Mandikal, P., V, R.M., Jamkhandi, A., RADHAKRISHNAN, V.B.: Cross-conditioned recurrent networks for long-term synthesis of

- inter-person human motion interactions. In: Proceedings of the IEEE/CVF Winter Conference on Applications of Computer Vision (WACV) (2020) **5, 7, 8, 16, 20, 21**
110. Kuo, C.F., Wang, M.J.J.: Motion generation and virtual simulation in a digital environment. *International Journal of Production Research* **50**(22), 6519–6529 (2012) **1**
 111. Kwon, P., Joo, H.: Graspdiffusion: Synthesizing realistic whole-body hand-object interaction. arXiv preprint arXiv:2410.13911 (2024) **5, 11, 22**
 112. Kwon, T., Tekin, B., Stühmer, J., Bogo, F., Pollefeys, M.: H2o: Two hands manipulating objects for first person interaction recognition. In: Proceedings of the IEEE/CVF International Conference on Computer Vision (ICCV), pp. 10138–10148 (2021) **11, 17**
 113. Lab, C.M.U.G.: Cmu graphics lab motion capture database (2003). URL <http://mocap.cs.cmu.edu/>. Accessed: 2024-11-01 **8, 16**
 114. Lee, G., Deng, Z., Ma, S., Shiratori, T., Srinivasa, S.S., Sheikh, Y.: Talking with hands 16.2m: A large-scale dataset of synchronized body-finger motion and audio for conversational motion analysis and synthesis. In: Proceedings of the IEEE/CVF International Conference on Computer Vision (ICCV) (2019) **16, 17**
 115. Lee, J., Joo, H.: Locomotion-action-manipulation: Synthesizing human-scene interactions in complex 3d environments. In: Proceedings of the IEEE/CVF International Conference on Computer Vision (ICCV) (2023) **13, 14**
 116. Lee, J., Saito, S., Nam, G., Sung, M., Kim, T.K.: Interhandgen: Two-hand interaction generation via cascaded reverse diffusion. In: Proceedings of the IEEE/CVF Conference on Computer Vision and Pattern Recognition, pp. 527–537 (2024) **5, 11**
 117. Li, J., Clegg, A., Mottaghi, R., Wu, J., Puig, X., Liu, C.K.: Controllable human-object interaction synthesis. In: European Conference on Computer Vision, pp. 54–72. Springer (2024) **10, 11**
 118. Li, J., Wu, J., Liu, C.K.: Object motion guided human motion synthesis. *ACM Transactions on Graphics (TOG)* **42**(6), 1–11 (2023) **5, 11, 17, 18**
 119. Li, L., Dai, A.: GenZI: Zero-shot 3D human-scene interaction generation. In: Proceedings of the IEEE/CVF Conference on Computer Vision and Pattern Recognition (CVPR) (2024) **13, 15**
 120. Li, Q., Wang, J., Loy, C.C., Dai, B.: Task-oriented human-object interactions generation with implicit neural representations. In: Proceedings of the IEEE/CVF Winter Conference on Applications of Computer Vision, pp. 3035–3044 (2024) **6, 11**
 121. Li, R., Yang, S., Ross, D.A., Kanazawa, A.: Ai choreographer: Music conditioned 3d dance generation with aist++. In: Proceedings of the IEEE/CVF International Conference on Computer Vision, pp. 13401–13412 (2021) **2**
 122. Li, X., Liu, S., Kim, K., Wang, X., Yang, M.H., Kautz, J.: Putting humans in a scene: Learning affordance in 3d indoor environments. In: IEEE Conference on Computer Vision and Pattern Recognition (2019) **13, 15**
 123. Li, Y., Lai, Z., Bao, W., Tan, Z., Dao, A., Sui, K., Shen, J., Liu, D., Liu, H., Kong, Y.: Visual large language models for generalized and specialized applications. arXiv preprint arXiv:2501.02765 (2025) **1**
 124. Liang, H., Zhang, W., Li, W., Yu, J., Xu, L.: Intergen: Diffusion-based multi-human motion generation under complex interactions. *International Journal of Computer Vision* (2024). DOI 10.1007/s11263-024-02042-6. URL <http://dx.doi.org/10.1007/s11263-024-02042-6> **4, 7, 8, 9, 10, 15, 16, 17, 21**
 125. Lim, D., Jeong, C., Kim, Y.M.: Mammos: Mapping multiple human motion with scene understanding and natural interactions. In: 2023 IEEE/CVF International Conference on Computer Vision Workshops (ICCVW), pp. 4280–4289 (2023). DOI 10.1109/ICCVW60793.2023.00462 **13**
 126. Lin, J., Guo, X., Shao, J., Jiang, C., Zhu, Y., Zhu, S.C.: A virtual reality platform for dynamic human-scene interaction. In: SIGGRAPH ASIA 2016 virtual reality meets physical reality: Modelling and simulating virtual humans and environments, pp. 1–4 (2016) **4**
 127. Liu, J., Shahroudy, A., Perez, M., Wang, G., Duan, L.Y., Kot, A.C.: Ntu rgb+d 120: A large-scale benchmark for 3d human activity understanding. *IEEE transactions on pattern analysis and machine intelligence* **42**(10), 2684–2701 (2019) **8, 16**
 128. Liu, S., Zhou, Y., Yang, J., Gupta, S., Wang, S.: Contactgen: Generative contact modeling for grasp generation. In: Proceedings of the IEEE/CVF International Conference on Computer Vision (ICCV), pp. 20609–20620 (2023) **11, 22**
 129. Liu, W., Bao, Q., Sun, Y., Mei, T.: Recent advances in monocular 2d and 3d human pose estimation: A deep learning perspective (2021). URL <https://arxiv.org/abs/2104.11536> **2**
 130. Liu, X., Hou, H., Yang, Y., Li, Y.L., Lu, C.: Revisit human-scene interaction via space occupancy. arXiv preprint arXiv:2312.02700 (2023) **5, 6, 13, 14**
 131. Liu, X., Yi, L.: Geneoh diffusion: Towards generalizable hand-object interaction denoising via denoising diffusion. In: The Twelfth International Conference on Learning Representations (2024) **11, 12, 22**
 132. Liu, Y., Liu, Y., Jiang, C., Lyu, K., Wan, W., Shen, H., Liang, B., Fu, Z., Wang, H., Yi, L.: Hoi4d: A 4d egocentric dataset for category-level human-object interaction. In: Proceedings of the IEEE/CVF Conference on Computer Vision and Pattern Recognition (CVPR), pp. 21013–21022 (2022) **11, 17**
 133. Liu, Y., Stoll, C., Gall, J., Seidel, H.P., Theobalt, C.: Markerless motion capture of interacting characters using multi-view image segmentation. In: CVPR 2011, pp. 1249–1256 (2011). DOI 10.1109/CVPR.2011.5995424 **16, 17**
 134. Loper, M., Mahmood, N., Romero, J., Pons-Moll, G., Black, M.J.: SMPL: A Skinned Multi-Person Linear Model, 1 edn. Association for Computing Machinery, New York, NY, USA (2023). URL <https://doi.org/10.1145/3596711.3596800> **3, 17**
 135. Lou, Z., Cui, Q., Wang, H., Tang, X., Zhou, H.: Multi-modal sense-informed prediction of 3d human motions. In: IEEE Conference on Computer Vision and Pattern Recognition (CVPR) (2024) **13, 15**
 136. Lucas, T., Baradel, F., Weinzaepfel, P., Rogez, G.: Posegpt: Quantization-based 3d human motion generation and forecasting. In: European Conference on Computer Vision, pp. 417–435. Springer (2022) **2**
 137. Lv, X., Xu, L., Yan, Y., Jin, X., Xu, C., Wu, S., Liu, Y., Li, L., Bi, M., Zeng, W., et al.: Himo: A new benchmark for full-body human interacting with multiple objects. *European Conference on Computer Vision* (2024) **10, 11, 17, 18**
 138. Maheshwari, S., Gupta, D., Sarvadevabhatla, R.K.: Mugl: Large scale multi person conditional action generation with locomotion (2021). URL <https://arxiv.org/abs/2110.11460> **5, 6, 8, 9, 20, 21**

139. Mahmood, N., Ghorbani, N., Troje, N.F., Pons-Moll, G., Black, M.J.: AMASS: Archive of motion capture as surface shapes. In: International Conference on Computer Vision, pp. 5442–5451 (2019) [8](#), [11](#), [13](#)
140. Makoviychuk, V., Wawrzyniak, L., Guo, Y., Lu, M., Storey, K., Macklin, M., Hoeller, D., Rudin, N., Allshire, A., Handa, A., State, G.: Isaac gym: High performance gpu-based physics simulation for robot learning (2021) [14](#)
141. von Marcard, T., Henschel, R., Black, M.J., Rosenhahn, B., Pons-Moll, G.: Recovering accurate 3d human pose in the wild using imus and a moving camera. In: Proceedings of the European Conference on Computer Vision (ECCV) (2018) [8](#), [16](#)
142. Mason, I., Starke, S., Komura, T.: Real-time style modelling of human locomotion via feature-wise transformations and local motion phases (2022). URL <https://arxiv.org/abs/2201.04439> [13](#)
143. McFee, B., Raffel, C., Liang, D., Ellis, D.P., McVicar, M., Battenberg, E., Nieto, O.: librosa: Audio and music signal analysis in python. In: SciPy, pp. 18–24 (2015) [4](#), [9](#)
144. Mehta, D., Sotnychenko, O., Mueller, F., Xu, W., Sridhar, S., Pons-Moll, G., Theobalt, C.: Single-shot multi-person 3d pose estimation from monocular rgb (2018). URL <https://arxiv.org/abs/1712.03453> [8](#), [16](#)
145. Men, Q., Shum, H.P.H., Ho, E.S.L., Leung, H.: GAN-based reactive motion synthesis with class-aware discriminators for human-human interaction (2021). URL <https://arxiv.org/abs/2110.00380> [5](#), [8](#)
146. Merriaux, P., Dupuis, Y., Boutteau, R., Vasseur, P., Savatier, X.: A study of vicon system positioning performance. *Sensors* **17**(7), 1591 (2017) [3](#)
147. Mihcin, S., Kose, H., Cizmeciogullari, S., Ciklacandir, S., Kocak, M., Tosun, A., Akan, A.: Investigation of wearable motion capture system towards biomechanical modelling. In: 2019 IEEE International Symposium on Medical Measurements and Applications (MeMeA), pp. 1–5. IEEE (2019) [3](#)
148. Milacski, Z.A., Niinuma, K., Kawamura, R., de la Torre, F., Jeni, L.A.: Ghost: Grounded human motion generation with open vocabulary scene-and-text contexts (2024). URL <https://arxiv.org/abs/2405.18438> [4](#), [6](#), [13](#), [15](#)
149. Mildenhall, B., Srinivasan, P.P., Tancik, M., Barron, J.T., Ramamoorthi, R., Ng, R.: Nerf: Representing scenes as neural radiance fields for view synthesis. *Communications of the ACM* **65**(1), 99–106 (2021) [1](#)
150. Minaee, S., Mikolov, T., Nikzad, N., Chenaghlu, M., Socher, R., Amatriain, X., Gao, J.: Large language models: A survey. *arXiv preprint arXiv:2402.06196* (2024) [1](#), [6](#)
151. Mir, A., Puig, X., Kanazawa, A., Pons-Moll, G.: Generating continual human motion in diverse 3d scenes (2023). URL <https://arxiv.org/abs/2304.02061> [13](#)
152. Monszpart, A., Guerrero, P., Ceylan, D., Yumer, E., J. Mitra, N.: iMapper: Interaction-guided scene mapping from monocular videos. *ACM SIGGRAPH* (2019) [18](#), [19](#)
153. Moon, G., Yu, S.I., Wen, H., Shiratori, T., Lee, K.M.: Interhand2. 6m: A dataset and baseline for 3d interacting hand pose estimation from a single rgb image. In: Computer Vision–ECCV 2020: 16th European Conference, Glasgow, UK, August 23–28, 2020, Proceedings, Part XX 16, pp. 548–564. Springer (2020) [11](#)
154. Mousas, C.: Performance-driven dance motion control of a virtual partner character. In: 2018 IEEE Conference on Virtual Reality and 3D User Interfaces (VR), pp. 57–64 (2018). DOI 10.1109/VR.2018.8446498 [5](#), [8](#)
155. Mullen Jr, J.F., Kothandaraman, D., Bera, A., Manocha, D.: Placing human animations into 3d scenes by learning interaction- and geometry-driven keyframes. *IEEE/CVF Winter Conference on Applications of Computer Vision (WACV)* (2023) [13](#)
156. Naksuk, N., Lee, C.G., Rietdyk, S.: Whole-body human-to-humanoid motion transfer. In: 5th IEEE-RAS International Conference on Humanoid Robots, 2005., pp. 104–109. IEEE (2005) [1](#)
157. Newcombe, R.A., Izadi, S., Hilliges, O., Molyneaux, D., Kim, D., Davison, A.J., Kohi, P., Shotton, J., Hodges, S., Fitzgibbon, A.: Kinectfusion: Real-time dense surface mapping and tracking. In: 2011 10th IEEE international symposium on mixed and augmented reality, pp. 127–136. Ieee (2011) [3](#)
158. Ng, E., Xiang, D., Joo, H., Grauman, K.: You2me: Inferring body pose in egocentric video via first and second person interactions (2020). URL <https://arxiv.org/abs/1904.09882> [16](#)
159. Norman, D.A.: The psychopathology of everyday things. In: Readings in human–computer interaction, pp. 5–21. Elsevier (1995) [1](#)
160. Pan, L., Wang, J., Huang, B., Zhang, J., Wang, H., Tang, X., Wang, Y.: Synthesizing physically plausible human motions in 3d scenes. In: International Conference on 3D Vision (3DV) (2024) [6](#), [13](#), [14](#)
161. Park, J.J., Florence, P., Straub, J., Newcombe, R., Lovegrove, S.: Deepsdf: Learning continuous signed distance functions for shape representation. In: Proceedings of the IEEE/CVF conference on computer vision and pattern recognition, pp. 165–174 (2019) [1](#)
162. Paschalidis, G., Wilschut, R., Antić, D., Taheri, O., Tzionas, D.: 3d whole-body grasp synthesis with directional controllability. *arXiv preprint arXiv:2408.16770* (2024) [11](#), [22](#)
163. Pavlakos, G., Choutas, V., Ghorbani, N., Bolkart, T., Osman, A.A.A., Tzionas, D., Black, M.J.: Expressive body capture: 3d hands, face, and body from a single image (2019). URL <https://arxiv.org/abs/1904.05866> [3](#), [17](#)
164. Peng, X., Xie, Y., Wu, Z., Jampani, V., Sun, D., Jiang, H.: Hoi-diff: Text-driven synthesis of 3d human-object interactions using diffusion models. *arXiv preprint arXiv:2312.06553* (2023) [10](#), [11](#)
165. Petrovich, M., Black, M.J., Varol, G.: Action-conditioned 3d human motion synthesis with transformer vae. In: Proceedings of the IEEE/CVF International Conference on Computer Vision, pp. 10985–10995 (2021) [2](#)
166. Petrovich, M., Black, M.J., Varol, G.: Temos: Generating diverse human motions from textual descriptions. In: European Conference on Computer Vision, pp. 480–497. Springer (2022) [2](#)
167. Pinyoanuntapong, E., Saleem, M.U., Karunratanakul, K., Wang, P., Xue, H., Chen, C., Guo, C., Cao, J., Ren, J., Tulyakov, S.: Controlmm: Controllable masked motion generation. *arXiv preprint arXiv:2410.10780* (2024) [24](#)
168. Plappert, M., Mandery, C., Asfour, T.: The KIT motion-language dataset. *Big Data* **4**(4), 236–252 (2016). DOI 10.1089/big.2016.0028. URL <http://dx.doi.org/10.1089/big.2016.0028> [8](#)
169. Ponce, P.R., Barquero, G., Palmero, C., Escalera, S., Garcia-Rodriguez, J.: in2in: Leveraging individual information to generate human interactions (2024). URL <https://arxiv.org/abs/2404.09988> [4](#), [8](#), [9](#), [20](#), [21](#), [22](#)

170. Prokudin, S., Lassner, C., Romero, J.: Efficient learning on point clouds with basis point sets. In: Proceedings of the IEEE/CVF international conference on computer vision, pp. 4332–4341 (2019) **4**, **10**, **14**
171. Puig, X., Ra, K., Boben, M., Li, J., Wang, T., Fidler, S., Torralba, A.: Virtualhome: Simulating household activities via programs. In: Proceedings of the IEEE conference on computer vision and pattern recognition, pp. 8494–8502 (2018) **4**
172. Punnakkal, A.R., Chandrasekaran, A., Athanasiou, N., Quiros-Ramirez, A., Black, M.J.: BABEL: Bodies, action and behavior with english labels. In: Proceedings IEEE/CVF Conf. on Computer Vision and Pattern Recognition (CVPR), pp. 722–731 (2021) **8**, **13**
173. Qi, C.R., Su, H., Mo, K., Guibas, L.J.: Pointnet: Deep learning on point sets for 3d classification and segmentation (2017). URL <https://arxiv.org/abs/1612.00593> **4**, **14**, **15**
174. Qu, H., Guo, Z., Liu, J.: Gpt-connect: Interaction between text-driven human motion generator and 3d scenes in a training-free manner (2024). URL <https://arxiv.org/abs/2403.14947> **13**, **15**
175. Radford, A., Kim, J.W., Hallacy, C., Ramesh, A., Goh, G., Agarwal, S., Sastry, G., Askell, A., Mishkin, P., Clark, J., et al.: Learning transferable visual models from natural language supervision. In: International conference on machine learning, pp. 8748–8763. PMLR (2021) **4**
176. Raffel, C., Shazeer, N., Roberts, A., Lee, K., Narang, S., Matena, M., Zhou, Y., Li, W., Liu, P.J.: Exploring the limits of transfer learning with a unified text-to-text transformer. *Journal of machine learning research* **21**(140), 1–67 (2020) **1**
177. Ramesh, A., Pavlov, M., Goh, G., Gray, S., Voss, C., Radford, A., Chen, M., Sutskever, I.: Zero-shot text-to-image generation. In: International conference on machine learning, pp. 8821–8831. Pmlr (2021) **1**
178. Rombach, R., Blattmann, A., Lorenz, D., Esser, P., Ommer, B.: High-resolution image synthesis with latent diffusion models. In: Proceedings of the IEEE/CVF conference on computer vision and pattern recognition, pp. 10684–10695 (2022) **1**
179. Romero, J., Tzionas, D., Black, M.J.: Embodied hands: Modeling and capturing hands and bodies together. *ACM Transactions on Graphics, (Proc. SIGGRAPH Asia)* **36**(6) (2017) **17**
180. Rumelhart, D.E., Hinton, G.E., Williams, R.J.: Learning representations by back-propagating errors. *nature* **323**(6088), 533–536 (1986) **5**
181. Ryoo, M.S., Aggarwal, J.K.: UT-Interaction Dataset, ICPR contest on Semantic Description of Human Activities (SDHA). http://cvrc.ece.utexas.edu/SDHA2010/Human_Interaction.html (2010) **8**, **16**
182. Savva, M., Chang, A.X., Hanrahan, P., Fisher, M., Nießner, M.: PiGraphs: Learning Interaction Snapshots from Observations. *ACM Transactions on Graphics (TOG)* **35**(4) (2016) **12**, **13**, **15**, **18**, **19**
183. Seitz, S.M., Curless, B., Diebel, J., Scharstein, D., Szeliski, R.: A comparison and evaluation of multi-view stereo reconstruction algorithms. In: 2006 IEEE computer society conference on computer vision and pattern recognition (CVPR'06), vol. 1, pp. 519–528. IEEE (2006) **3**
184. Shafir, Y., Tevet, G., Kapon, R., Bermano, A.H.: Human motion diffusion as a generative prior (2023). URL <https://arxiv.org/abs/2303.01418> **4**, **8**, **9**, **20**, **21**
185. Shan, M., Dong, L., Han, Y., Yao, Y., Liu, T., Nwogu, I., Qi, G.J., Hill, M.: Towards open domain text-driven synthesis of multi-person motions (2024). URL <https://arxiv.org/abs/2405.18483> **4**, **6**, **7**, **8**, **9**, **16**, **17**
186. Shen, Y., Yang, L., Ho, E.S.L., Shum, H.P.H.: Interaction-based human activity comparison. *IEEE Transactions on Visualization and Computer Graphics* **26**(8), 2620–2633 (2020). DOI 10.1109/TVCG.2019.2893247 **8**, **16**
187. Shi, J., et al.: Good features to track. In: 1994 Proceedings of IEEE conference on computer vision and pattern recognition, pp. 593–600. IEEE (1994) **3**
188. Shimada, S., Mueller, F., Bednarik, J., Doosti, B., Bickel, B., Tang, D., Golyanik, V., Taylor, J., Theobalt, C., Beeler, T.: Macs: Mass conditioned 3d hand and object motion synthesis. In: International Conference on 3D Vision (3DV) (2024) **11**
189. Shu, T., Ryoo, M.S., Zhu, S.C.: Learning social affordance for human-robot interaction (2016). URL <https://arxiv.org/abs/1604.03692> **8**, **15**, **19**
190. Singer, U., Polyak, A., Hayes, T., Yin, X., An, J., Zhang, S., Hu, Q., Yang, H., Ashual, O., Gafni, O., et al.: Make-a-video: Text-to-video generation without text-video data. arXiv preprint arXiv:2209.14792 (2022) **1**
191. Siyao, L., Gu, T., Yang, Z., Lin, Z., Liu, Z., Ding, H., Yang, L., Loy, C.C.: Duolando: Follower gpt with off-policy reinforcement learning for dance accompaniment (2024). URL <https://arxiv.org/abs/2403.18811> **4**, **6**, **7**, **8**, **9**, **10**, **16**, **17**, **20**, **21**, **22**
192. Siyao, L., Yu, W., Gu, T., Lin, C., Wang, Q., Qian, C., Loy, C.C., Liu, Z.: Bailando: 3d dance generation by actor-critic gpt with choreographic memory. In: Proceedings of the IEEE/CVF Conference on Computer Vision and Pattern Recognition, pp. 11050–11059 (2022) **2**, **20**, **22**
193. Sohn, K., Lee, H., Yan, X.: Learning structured output representation using deep conditional generative models. *Advances in neural information processing systems* **28** (2015) **6**
194. Sridhar, S., Mueller, F., Zollhoefer, M., Casas, D., Oulasvirta, A., Theobalt, C.: Real-time joint tracking of a hand manipulating an object from rgb-d input. In: Proceedings of European Conference on Computer Vision (ECCV) (2016). URL <http://handtracker.mpi-inf.mpg.de/projects/RealtimEHO/> **17**
195. Starke, S., Zhang, H., Komura, T., Saito, J.: Neural state machine for character-scene interactions. *ACM Transactions on Graphics* **38**(6), 178 (2019) **5**
196. Starke, S., Zhang, H., Komura, T., Saito, J.: Neural state machine for character-scene interactions. *ACM Trans. Graph.* **38**(6) (2019). DOI 10.1145/3355089.3356505. URL <https://doi.org/10.1145/3355089.3356505> **13**, **15**
197. Starke, S., Zhao, Y., Komura, T., Zaman, K.: Local motion phases for learning multi-contact character movements. *ACM Transactions on Graphics (TOG)* **39**(4), 54–1 (2020) **5**, **8**, **23**
198. Starke, S., Zhao, Y., Zinno, F., Komura, T.: Neural animation layering for synthesizing martial arts movements. *ACM Transactions on Graphics (TOG)* **40**(4), 1–16 (2021) **5**, **8**, **23**
199. Surmen, H.K.: Photogrammetry for 3d reconstruction of objects: Effects of geometry, texture and photographing. *Image Analysis and Stereology* **42**(2), 51–63 (2023) **3**
200. Taheri, O., Choutas, V., Black, M.J., Tzionas, D.: GOAL: Generating 4D whole-body motion for hand-object grasping. In: Conference on Computer Vision and Pattern

- Recognition (CVPR) (2022). URL <https://goal.is.tue.mpg.de> 10, 11
201. Taheri, O., Ghorbani, N., Black, M.J., Tzionas, D.: Grab: A dataset of whole-body human grasping of objects. In: Computer Vision—ECCV 2020: 16th European Conference, Glasgow, UK, August 23–28, 2020, Proceedings, Part IV 16, pp. 581–600. Springer (2020) 11, 17, 18
 202. Taheri, O., Zhou, Y., Tzionas, D., Zhou, Y., Ceylan, D., Pirk, S., Black, M.J.: GRIP: Generating interaction poses using latent consistency and spatial cues. In: International Conference on 3D Vision (3DV) (2024) 5, 10, 11
 203. Tanaka, M., Fujiwara, K.: Role-aware interaction generation from textual description. In: Proceedings of the IEEE/CVF International Conference on Computer Vision (ICCV), pp. 15999–16009 (2023) 8, 9, 20, 21
 204. Tang, J., Jingya, W., Ji, K., Xu, L., Yu, J., Shi, Y.: A unified diffusion framework for scene-aware human motion estimation from sparse signals. arXiv preprint arXiv:2404.04890 (2024) 13, 14
 205. Tanke, J., Zaveri, C., Gall, J.: Intention-based long-term human motion anticipation. In: International Conference on 3D Vision (2021) 20
 206. Tanke, J., Zhang, L., Zhao, A., Tang, C., Cai, Y., Wang, L., Wu, P.C., Gall, J., Keskin, C.: Social diffusion: Long-term multiple human motion anticipation. In: 2023 IEEE/CVF International Conference on Computer Vision (ICCV), pp. 9567–9577 (2023). DOI 10.1109/ICCV51070.2023.00880 8, 20
 207. Tendulkar, P., Surís, D., Vondrick, C.: Flex: Full-body grasping without full-body grasps. In: Proceedings of the IEEE/CVF Conference on Computer Vision and Pattern Recognition, pp. 21179–21189 (2023) 11
 208. Tevet, G., Raab, S., Cohan, S., Reda, D., Luo, Z., Peng, X.B., Bermano, A.H., van de Panne, M.: Closs: Closing the loop between simulation and diffusion for multi-task character control. arXiv preprint arXiv:2410.03441 (2024) 13, 14
 209. Tevet, G., Raab, S., Gordon, B., Shafir, Y., Cohen-or, D., Bermano, A.H.: Human motion diffusion model. In: The Eleventh International Conference on Learning Representations (2023). URL <https://openreview.net/forum?id=SJ1kSy02jwu> 2
 210. Tevet, G., Raab, S., Gordon, B., Shafir, Y., Cohen-or, D., Bermano, A.H.: Human motion diffusion model. In: The Eleventh International Conference on Learning Representations (2023). URL <https://openreview.net/forum?id=SJ1kSy02jwu> 9
 211. Touvron, H., Lavril, T., Izacard, G., Martinet, X., Lachaux, M.A., Lacroix, T., Rozière, B., Goyal, N., Hambro, E., Azhar, F., et al.: Llama: Open and efficient foundation language models. arXiv preprint arXiv:2302.13971 (2023) 1
 212. Tran, D., Bourdev, L., Fergus, R., Torresani, L., Paluri, M.: Learning spatiotemporal features with 3d convolutional networks. In: Proceedings of the IEEE international conference on computer vision, pp. 4489–4497 (2015) 4
 213. Tseng, J., Castellon, R., Liu, K.: Edge: Editable dance generation from music. In: Proceedings of the IEEE/CVF Conference on Computer Vision and Pattern Recognition, pp. 448–458 (2023) 2
 214. Tulyakov, S., Liu, M.Y., Yang, X., Kautz, J.: Mocogan: Decomposing motion and content for video generation. In: Proceedings of the IEEE conference on computer vision and pattern recognition, pp. 1526–1535 (2018) 1
 215. Ugrinovic, N., Lucas, T., Baradel, F., Weinzaepfel, P., Rogez, G., Moreno-Noguer, F.: Purposer: Putting human motion generation in context (2024) 5, 6, 13, 15
 216. Van Den Oord, A., Dieleman, S., Zen, H., Simonyan, K., Vinyals, O., Graves, A., Kalchbrenner, N., Senior, A., Kavukcuoglu, K., et al.: Wavenet: A generative model for raw audio. arXiv preprint arXiv:1609.03499 12 (2016) 1
 217. Van Den Oord, A., Vinyals, O., et al.: Neural discrete representation learning. Advances in neural information processing systems 30 (2017) 6
 218. Van Welbergen, H., Van Basten, B.J., Egges, A., Ruttkay, Z.M., Overmars, M.H.: Real time animation of virtual humans: a trade-off between naturalness and control. In: Computer Graphics Forum, vol. 29, pp. 2530–2554. Wiley Online Library (2010) 1
 219. Vaswani, A., Shazeer, N., Parmar, N., Uszkoreit, J., Jones, L., Gomez, A.N., Kaiser, L., Polosukhin, I.: Attention is all you need (2023). URL <https://arxiv.org/abs/1706.03762> 5, 6
 220. de la Vega-Hazas, L., Calatayud, F., Iglesias, A.: Applying evolutionary computation operators for automatic human motion generation in computer animation and video games. In: Intelligent Distributed Computing XII, pp. 247–258. Springer (2018) 1
 221. Vendrow, E., Kumar, S., Adeli, E., Rezaatofghi, H.: Somformer: Multi-person pose forecasting with transformers (2022). URL <https://arxiv.org/abs/2208.14023> 8, 9
 222. Villegas, R., Yang, J., Ceylan, D., Lee, H.: Neural kinematic networks for unsupervised motion retargetting. In: Proceedings of the IEEE conference on computer vision and pattern recognition, pp. 8639–8648 (2018) 3
 223. Vondrick, C., Pirsiaavash, H., Torralba, A.: Generating videos with scene dynamics. Advances in neural information processing systems 29 (2016) 1
 224. Wang, H., Zhu, W., Miao, L., Xu, Y., Gao, F., Tian, Q., Wang, Y.: Aligning motion generation with human perceptions. In: International Conference on Learning Representations (ICLR) (2025) 20, 21
 225. Wang, J., Rong, Y., Liu, J., Yan, S., Lin, D., Dai, B.: Towards diverse and natural scene-aware 3d human motion synthesis. 2022 IEEE/CVF Conference on Computer Vision and Pattern Recognition (CVPR) pp. 20428–20437 (2022). URL <https://api.semanticscholar.org/CorpusID:248913210> 13, 14
 226. Wang, J., Xu, H., Narasimhan, M., Wang, X.: Multi-person 3d motion prediction with multi-range transformers (2021). URL <https://arxiv.org/abs/2111.12073> 8, 20, 23
 227. Wang, J., Xu, H., Xu, J., Liu, S., Wang, X.: Synthesizing long-term 3d human motion and interaction in 3d scenes (2020) 12, 13, 14
 228. Wang, R., Mao, W., Li, H.: DeepsimHO: Stable pose estimation for hand-object interaction via physics simulation. In: Thirty-seventh Conference on Neural Information Processing Systems (2023). URL <https://openreview.net/forum?id=SxVHyYavHy> 4
 229. Wang, W., Pan, L., Dou, Z., Liao, Z., Lou, Y., Yang, L., Wang, J., Komura, T.: Sims: Simulating human-scene interactions with real world script planning (2024). URL <https://arxiv.org/abs/2411.19921> 6, 13, 14
 230. Wang, Y., Guo, C., Cheng, L., Jiang, H.: Regiongrasp: A novel task for contact region controllable hand grasp generation. arXiv preprint arXiv:2410.07995 (2024) 11
 231. Wang, Y., Lin, J., Zeng, A., Luo, Z., Zhang, J., Zhang, L.: Physhoi: Physics-based imitation of dynamic human-object interaction. arXiv preprint arXiv:2312.04393 (2023) 4

232. Wang, Y., Wang, Z., Liu, L., Daniilidis, K.: Tram: Global trajectory and motion of 3d humans from in-the-wild videos. In: European Conference on Computer Vision, pp. 467–487. Springer (2024) **3**
233. Wang, Z., Chen, Y., Jia, B., Li, P., Zhang, J., Zhang, J., Liu, T., Zhu, Y., Liang, W., Huang, S.: Move as you say, interact as you can: Language-guided human motion generation with scene affordance. In: Proceedings of the IEEE/CVF Conference on Computer Vision and Pattern Recognition (CVPR) (2024) **6, 13, 14**
234. Wang, Z., Chen, Y., Liu, T., Zhu, Y., Liang, W., Huang, S.: Humanise: Language-conditioned human motion generation in 3d scenes. In: Advances in Neural Information Processing Systems (NeurIPS) (2022) **4, 13, 18, 19**
235. Wang, Z., Wang, J., Li, Y., Lin, D., Dai, B.: Intercontrol: Zero-shot human interaction generation by controlling every joint (2024). URL <https://arxiv.org/abs/2311.15864> **4, 5, 8, 9, 10, 20, 21, 23**
236. Wu, J., Zhang, C., Xue, T., Freeman, B., Tenenbaum, J.: Learning a probabilistic latent space of object shapes via 3d generative-adversarial modeling. *Advances in neural information processing systems* **29** (2016) **1**
237. Wu, T., Pan, L., Zhang, J., Wang, T., Liu, Z., Lin, D.: Balanced chamfer distance as a comprehensive metric for point cloud completion. *Advances in Neural Information Processing Systems* **34**, 29088–29100 (2021) **11, 20, 22**
238. Wu, Y., Wang, J., Zhang, Y., Zhang, S., Hilliges, O., Yu, F., Tang, S.: Saga: Stochastic whole-body grasping with contact. In: Proceedings of the European Conference on Computer Vision (ECCV) (2022) **10, 11**
239. Xiang, Y., Schmidt, T., Narayanan, V., Fox, D.: Posecnn: A convolutional neural network for 6d object pose estimation in cluttered scenes. *arXiv preprint arXiv:1711.00199* (2017) **3**
240. Xiao, Z., Wang, T., Wang, J., Cao, J., Zhang, W., Dai, B., Lin, D., Pang, J.: Unified human-scene interaction via prompted chain-of-contacts. In: The Twelfth International Conference on Learning Representations (2024). URL <https://openreview.net/forum?id=1vCnDyQkjg> **6, 13, 14, 15, 23**
241. Xie, Y., Jampani, V., Zhong, L., Sun, D., Jiang, H.: Omnicontrol: Control any joint at any time for human motion generation. *arXiv preprint arXiv:2310.08580* (2023) **24**
242. Xing, C., Mao, W., Liu, M.: Scene-aware human motion forecasting via mutual distance prediction (2024). URL <https://arxiv.org/abs/2310.00615> **13, 14**
243. Xu, H., Bazavan, E.G., Zanfir, A., Freeman, W.T., Sukthankar, R., Sminchisescu, C.: Ghum & ghuml: Generative 3d human shape and articulated pose models. In: Proceedings of the IEEE/CVF Conference on Computer Vision and Pattern Recognition (CVPR) (2020) **3, 17**
244. Xu, L., Lv, X., Yan, Y., Jin, X., Wu, S., Xu, C., Liu, Y., Zhou, Y., Rao, F., Sheng, X., Liu, Y., Zeng, W., Yang, X.: Inter-x: Towards versatile human-human interaction analysis (2023). URL <https://arxiv.org/abs/2312.16051> **3, 7, 15, 16, 17**
245. Xu, L., Song, Z., Wang, D., Su, J., Fang, Z., Ding, C., Gan, W., Yan, Y., Jin, X., Yang, X., Zeng, W., Wu, W.: Actformer: A gan-based transformer towards general action-conditioned 3d human motion generation (2022). URL <https://arxiv.org/abs/2203.07706> **5, 8, 16, 21**
246. Xu, L., Zhou, Y., Yan, Y., Jin, X., Zhu, W., Rao, F., Yang, X., Zeng, W.: Regennet: Towards human action-reaction synthesis (2024). URL <https://arxiv.org/abs/2403.11882> **8, 9, 21**
247. Xu, S., Li, Z., Wang, Y.X., Gui, L.Y.: Interdiff: Generating 3d human-object interactions with physics-informed diffusion. In: Proceedings of the IEEE/CVF International Conference on Computer Vision, pp. 14928–14940 (2023) **3, 11, 23**
248. Xu, S., Wang, Z., Wang, Y.X., Gui, L.Y.: Interdreamer: Zero-shot text to 3d dynamic human-object interaction. *The Thirty-Eighth Annual Conference on Neural Information Processing Systems* (2024) **6, 11**
249. Xuan, H., Li, X., Zhang, J., Zhang, H., Liu, Y., Li, K.: Narrator: Towards natural control of human-scene interaction generation via relationship reasoning. In: *arXiv preprint arXiv:2303.09410* (2023) **6, 13, 14, 15**
250. Yang, J., Niu, X., Jiang, N., Zhang, R., Siyuan, H.: F-hoi: Toward fine-grained semantic-aligned 3d human-object interactions. *European Conference on Computer Vision* (2024) **4, 10, 11, 17, 18**
251. Yang, L., Li, K., Zhan, X., Wu, F., Xu, A., Liu, L., Lu, C.: Oakink: A large-scale knowledge repository for understanding hand-object interaction. In: Proceedings of the IEEE/CVF conference on computer vision and pattern recognition, pp. 20953–20962 (2022) **11**
252. Yang, L., Zhang, Z., Song, Y., Hong, S., Xu, R., Zhao, Y., Zhang, W., Cui, B., Yang, M.H.: Diffusion models: A comprehensive survey of methods and applications. *ACM Computing Surveys* **56**(4), 1–39 (2023) **1**
253. Yang, Y., Yang, J., Hodgins, J.: Statistics-based motion synthesis for social conversations. In: Proceedings of the 2020 ACM SIGGRAPH/Eurographics symposium on Computer animation (2020) **4, 5, 8, 9**
254. Ye, Y., Gupta, A., Kitani, K., Tulsiani, S.: G-hop: Generative hand-object prior for interaction reconstruction and grasp synthesis. In: *CVPR* (2024) **11, 12**
255. Yi, H., Thies, J., Black, M.J., Peng, X.B., Rempe, D.: Generating human interaction motions in scenes with text control. *arXiv:2404.10685* (2024) **6, 13**
256. Yin, Y., Guo, C., Kaufmann, M., Zarate, J.J., Song, J., Hilliges, O.: Hi4d: 4d instance segmentation of close human interaction (2023). URL <https://arxiv.org/abs/2303.15380> **16, 17**
257. Yun, K., Honorio, J., Chattopadhyay, D., Berg, T., Samaras, D.: Two-person interaction detection using body-pose features and multiple instance learning. pp. 28–35 (2012). DOI 10.1109/CVPRW.2012.6239234 **8, 16**
258. Zhang, H., Christen, S., Fan, Z., Zheng, L., Hwangbo, J., Song, J., Hilliges, O.: Artigrasp: Physically plausible synthesis of bi-manual dexterous grasping and articulation. In: 2024 International Conference on 3D Vision (3DV), pp. 235–246. IEEE (2024) **5, 6, 11, 12**
259. Zhang, H., Ye, Y., Shiratori, T., Komura, T.: Manipnet: neural manipulation synthesis with a hand-object spatial representation. *ACM Transactions on Graphics (ToG)* **40**(4), 1–14 (2021) **11, 12**
260. Zhang, J., Luo, H., Yang, H., Xu, X., Wu, Q., Shi, Y., Yu, J., Xu, L., Wang, J.: Neurdome: A neural modeling pipeline on multi-view human-object interactions. In: *CVPR* (2023) **11, 17, 18**
261. Zhang, J., Zhang, J., Song, Z., Shi, Z., Zhao, C., Shi, Y., Yu, J., Xu, L., Wang, J.: Hoi-m3: capture multiple humans and objects interaction within contextual environment (2024). URL <https://arxiv.org/abs/2404.00299> **15, 19**
262. Zhang, J., Zhang, Y., Cun, X., Zhang, Y., Zhao, H., Lu, H., Shen, X., Shan, Y.: Generating human motion from textual descriptions with discrete representations. In: Proceedings of the IEEE/CVF conference on computer

- vision and pattern recognition, pp. 14730–14740 (2023) [2](#)
263. Zhang, L., Rao, A., Agrawala, M.: Adding conditional control to text-to-image diffusion models (2023). URL <https://arxiv.org/abs/2302.05543> [9](#)
264. Zhang, M., Fu, Y., Ding, Z., Liu, S., Tu, Z., Wang, X.: Hoidiffusion: Generating realistic 3d hand-object interaction data. In: Proceedings of the IEEE/CVF Conference on Computer Vision and Pattern Recognition, pp. 8521–8531 (2024) [6](#), [10](#), [11](#)
265. Zhang, S.: High-speed 3d shape measurement with structured light methods: A review. *Optics and lasers in engineering* **106**, 119–131 (2018) [3](#)
266. Zhang, S., Ma, Q., Zhang, Y., Qian, Z., Kwon, T., Pollefeys, M., Bogó, F., Tang, S.: Egobody: Human body shape and motion of interacting people from head-mounted devices. In: European Conference on Computer Vision, pp. 180–200. Springer (2022) [18](#), [19](#)
267. Zhang, S., Zhang, Y., Bogó, F., Pollefeys, M., Tang, S.: Learning motion priors for 4d human body capture in 3d scenes. In: Proceedings of the IEEE/CVF International Conference on Computer Vision, pp. 11343–11353 (2021) [13](#)
268. Zhang, S., Zhang, Y., Ma, Q., Black, M.J., Tang, S.: Place: Proximity learning of articulation and contact in 3d environments. In: 2020 International Conference on 3D Vision (3DV), pp. 642–651. IEEE (2020) [13](#), [14](#)
269. Zhang, X., Bhatnagar, B.L., Starke, S., Guzov, V., Pons-Moll, G.: Couch: Towards controllable human-chair interactions. In: European Conference on Computer Vision, pp. 518–535. Springer (2022) [10](#), [17](#), [18](#)
270. Zhang, X., Bhatnagar, B.L., Starke, S., Petrov, I., Guzov, V., Dharmo, H., Pérez Pellitero, E., Pons-Moll, G.: Force: Dataset and method for intuitive physics guided human-object interaction. arxiv preprint (2024) [4](#)
271. Zhang, Y., Hassan, M., Neumann, H., Black, M.J., Tang, S.: Generating 3d people in scenes without people. In: Computer Vision and Pattern Recognition (CVPR) (2020). URL <https://arxiv.org/abs/1912.02923> [13](#), [14](#)
272. Zhang, Y., Tang, S.: The wanderings of odysseus in 3d scenes. In: Proceedings of the IEEE/CVF Conference on Computer Vision and Pattern Recognition, pp. 20481–20491 (2022) [13](#), [14](#)
273. Zhang, Z.: Microsoft kinect sensor and its effect. *IEEE multimedia* **19**(2), 4–10 (2012) [3](#)
274. Zhao, C., Zhang, J., Du, J., Shan, Z., Wang, J., Yu, J., Wang, J., Xu, L.: I’m hoi: Inertia-aware monocular capture of 3d human-object interactions. In: Proceedings of the IEEE/CVF Conference on Computer Vision and Pattern Recognition, pp. 729–741 (2024) [11](#), [17](#), [18](#)
275. Zhao, H., Jiang, L., Jia, J., Torr, P.H., Koltun, V.: Point transformer. In: Proceedings of the IEEE/CVF International Conference on Computer Vision, pp. 16259–16268 (2021) [4](#)
276. Zhao, K., Wang, S., Zhang, Y., Beeler, T., , Tang, S.: Compositional human-scene interaction synthesis with semantic control. In: European conference on computer vision (ECCV) (2022) [13](#), [14](#), [15](#), [20](#), [22](#)
277. Zhao, K., Zhang, Y., Wang, S., Beeler, T., , Tang, S.: Synthesizing diverse human motions in 3d indoor scenes. In: International conference on computer vision (ICCV) (2023) [5](#), [13](#), [14](#), [20](#), [22](#)
278. Zheng, J., Zheng, Q., Fang, L., Liu, Y., Yi, L.: Cams: Canonicalized manipulation spaces for category-level functional hand-object manipulation synthesis. In: Proceedings of the IEEE/CVF Conference on Computer Vision and Pattern Recognition (CVPR), pp. 585–594 (2023) [11](#)
279. Zheng, Y., Shao, R., Zhang, Y., Yu, T., Zheng, Z., Dai, Q., Liu, Y.: Deepmulticap: Performance capture of multiple characters using sparse multiview cameras (2021). URL <https://arxiv.org/abs/2105.00261> [16](#), [17](#)
280. Zheng, Y., Yang, Y., Mo, K., Li, J., Yu, T., Liu, Y., Liu, K., Guibas, L.J.: Gimo: Gaze-informed human motion prediction in context. arXiv preprint arXiv:2204.09443 (2022) [13](#), [18](#), [19](#)
281. Zhong, L., Xie, Y., Jampani, V., Sun, D., Jiang, H.: Smoodi: Stylized motion diffusion model. In: European Conference on Computer Vision, pp. 405–421. Springer (2024) [24](#)
282. Zhou, K., Bhatnagar, B.L., Lenssen, J.E., Pons-Moll, G.: Toch: Spatio-temporal object-to-hand correspondence for motion refinement. In: European Conference on Computer Vision (ECCV). Springer (2022) [11](#)
283. Zhou, K., Bhatnagar, B.L., Lenssen, J.E., Pons-Moll, G.: Gears: Local geometry-aware hand-object interaction synthesis. In: Proceedings of the IEEE/CVF Conference on Computer Vision and Pattern Recognition, pp. 20634–20643 (2024) [5](#), [11](#), [12](#)
284. Zhou, Y., Barnes, C., Lu, J., Yang, J., Li, H.: On the continuity of rotation representations in neural networks. In: Proceedings of the IEEE/CVF conference on computer vision and pattern recognition, pp. 5745–5753 (2019) [3](#)
285. Zhu, W., Ma, X., Ro, D., Ci, H., Zhang, J., Shi, J., Gao, F., Tian, Q., Wang, Y.: Human motion generation: A survey (2023). URL <https://arxiv.org/abs/2307.10894> [2](#)
286. Zollhöfer, M., Stotko, P., Görllitz, A., Theobalt, C., Nießner, M., Klein, R., Kolb, A.: State of the art on 3d reconstruction with rgb-d cameras. In: Computer graphics forum, vol. 37, pp. 625–652. Wiley Online Library (2018) [3](#)
287. Zuo, B., Zhao, Z., Sun, W., Yuan, X., Yu, Z., Wang, Y.: Graspdiff: Grasping generation for hand-object interaction with multimodal guided diffusion. *IEEE Transactions on Visualization and Computer Graphics* (2024) [11](#), [20](#), [22](#)